Exosomes can modulate the early hyperexcitability in cortical neurons with ASD-associated *Shank3* mutation.

Ashwani Choudhary[1,*], Idan Rosh[1,*], Yara Hussein[1], Aviram Shemen[1], Wote Amelo Rike [1], Assaf Zinger[2], Daniel Offen[3,4], Shani Stern[1,#]

[1]Sagol Department of Neurobiology, Faculty of Natural Sciences, University of Haifa, Haifa 3498838, Israel

[2]Department of Chemical Engineering, Technion - Israel Institute of Technology, Haifa, 32000, Israel

[3]Sagol School of Neuroscience, Tel Aviv University, Tel Aviv 69978, Israel

[4]Department of Human Molecular Genetics and Biochemistry, Felsenstein Medical Research Center, Sackler School of Medicine, Tel Aviv University, Tel Aviv 69978, Israel

*Equally contributing authors

#Correspondence: Shani Stern, sstern@univ.haifa.ac.il

ABSTRACT:

Shank3, a scaffolding protein, is critical for synaptic structure and function, particularly for the formation and maintenance of dendritic spines. *Shank3* mutations are strongly implicated in autism spectrum disorder (ASD) and related neuropsychiatric conditions such as Phelan-McDermid Syndrome (PMS) also known as the 22q13.3 deletion syndrome. Previous work has recognized early hyperexcitability in cortical neurons derived from ASD patients with various gene mutations as a potential common endophenotype. In this study, we examined the effects of exosomes extracted from several cell types on the neurophysiological properties of cortical neurons derived from *Shank3* (c.3679insG mutation) induced pluripotent stem cells (iPSCs). First, we sought to understand the implications of exosome-based intercellular communication on the neurophysiology of *Shank3* mutant and control neurons by switching their respective exosomes. We found that while control neuron-derived exosomes do not change the neurophysiology of *Shank3* neurons, the *Shank3* neuron-derived exosomes transfer the early hyperexcitability and other ASD-related phenotypes to control neurons. Next, we also explored the therapeutic potential of mesenchymal stem cells (MSC) and iPSC-derived exosomes from healthy donors in the *Shank3* cortical neurons. We demonstrate that both MSC and iPSC-derived exosomes rescue the early hyperexcitability and accelerated maturation of *Shank3* neurons. Proteomic analysis of exosomes derived from *Shank3* mutant and control neurons, as well as from exosomes derived from MSCs and iPSCs, revealed distinct protein cargoes that may cause changes in the neurophysiological properties of the recipient neurons. Our results hence provide novel insights into the pathophysiology of ASD emphasizing the importance of exosomes in intercellular communication and their potential to influence intrinsic and network properties of neurons. Moreover, our findings support the need for further exploration of exosome-based interventions as potential therapeutics for treating neurodevelopmental disorders.

INTRODUCTION:

The *Shank3* gene belongs to the family of ProSAP/Shank genes [1,2] and plays a key role in maintaining synaptic plasticity which is essential for fundamental processes like cognition, memory, and learning[3]. The Shank family genes function as a master scaffolding protein in the post-synaptic density of excitatory neurons assembling the PSD-95 protein (postsynaptic density-95), NMDA receptors, AMPA receptors, and homer-based complexes[2,4]. The impairment of *Shank3* function has been primarily associated with PMS[5]. PMS or the 22q13.3 deletion syndrome is a neurodevelopmental condition caused by a deletion of the region spanning the *Shank3* gene (distal arm of Chromosome 22) [6]. PMS is characterized by delayed speech and language development, ASD-like symptoms, intellectual disabilities (ID), and other behavioral abnormalities[6,7]. Some PMS patients exhibit symptoms identical to those reported in patients with haploinsufficiency of *Shank3* mutations, implying a clear causal relationship between *Shank3* function loss and the manifestation of specific neurodevelopmental symptoms in PMS patients[7].

Apart from PMS, several studies have also implicated point mutations in *Shank3* in ASDs, IDs, and Schizophrenia (SCZ) patients [8,9]. Mutations in the *Shank3* gene are strongly associated with ASD with estimates of approximately 1% of the incidence in ASD patients[10]. Moreover, transgenic mice models with a *Shank3* knockout or loss of function exhibit ASD symptoms such as decreased social interactions, repetitive behaviors, cognitive deficits, and synaptic dysfunction[11,12]. We recently generated iPSCs from a PMS patient with a *Shank3* mutation (c.3679insG)[13] and reported the neurophysiological properties of iPSC-derived cortical neurons[14]. Our results demonstrated that cortical neurons with this *Shank3* mutation, similar to several other ASD-associated mutations, displayed early maturation and hyperexcitability in comparison to unaffected healthy neurons. The hyperexcitability due to *Shank3* haploinsufficiency was also reported by another group in human embryonic stem cell-derived glutamatergic neurons as well as in mouse primary hippocampal neurons harboring *Shank3*

deletion [15]. Hyperactivity of the corticostriatal circuit and abnormal maturation were also observed during the early development of *Shank3B*$^{-/-}$ mice displaying autistic characteristics [16].

In recent years, exosomes and their role in neurological disorders have emerged as a novel area of research. Exosomes are membrane-bound, nano-sized (50-200nm) vesicles released primarily by eukaryotic cell types, including neural cells[17]. Exosomes transport a wide range of proteins, lipids, and nucleic acids from the parent cells, making them useful intercellular communication players under both healthy and diseased conditions [18]. Several reports have emphasized the role of exosomes as mediators of signaling molecules during immunological and inflammatory cellular responses[19]. Exosomes have also been reported to transport misfolded or aggregated proteins associated with neurodegenerative diseases such as Alzheimer's disease (AD), Parkinson's disease (PD), and amyotrophic lateral sclerosis (ALS) to the recipient cells leading to the dissemination of pathological features [20]. Previous research has also documented the beneficial properties of exosomes by demonstrating that exosomes originating from oligodendrocytes enhance neuronal survival under conditions of cellular stress[21,22]. Stem cells, notably mesenchymal stem cells (MSCs) and iPSC-derived exosomes have garnered significant interest due to their therapeutic potential[23,24]. Unlike stem cell transplantation therapies, exosomes derived from these cells are generally non-immunogenic, can be administered via multiple routes (intranasal, intravenous, nebulizer), and pose minimal ethical concerns[25]. However, despite multiple pieces of evidence, the therapeutic application of exosomes is largely limited for neurological disorders majorly due to the lack of preclinical studies in human cells[26]. Moreover, the mechanisms by which the exosomes impart their neuroprotective effect are underexplored.

In this study, we have used an iPSC model of the c.3679insG *Shank3* mutation and performed a functional analysis of cortical neurons by electrophysiology. We hypothesized that the hyperexcitability phenotype of *Shank3* neurons might be mediated by exosomes and hence performed an exosome exchange. We purified exosomes from control cortical neurons and these were applied to the *Shank3* mutant (c.3679insG) cortical neurons and vice versa. We

discovered that when treating control neurons with *Shank3* exosomes, they exhibited properties like *Shank3* neurons with an increased total evoked potential and spontaneous firing rate while the *Shank3* neurons treated with control exosomes were not altered. In addition, to test the therapeutic potential of stem cell-derived exosomes, we treated the *Shank3* mutant cortical neurons with exosomes derived from MSCs (MSC-exo) and iPSCs (iPSC-exo) both from healthy control donors. We found that both MSC-exo and iPSC-exo were able to rescue the abnormal electrophysiological properties of *Shank3* mutant cortical neurons, making them similar to control neurons. Furthermore, we conducted proteomic analysis of exosomes derived from *Shank3* mutant neurons, control neurons, MSC-exo, and iPSC-exo to explore the protein cargo contributing to the distinct physiological effects observed in our experiments. Overall, our study shows that exosomes can modulate the neurophysiological properties of human neural cells. Additionally, we demonstrate that MSC-derived exosomes (MSC-exo) and control iPSC-derived exosomes (iPSC-exo) can reverse the abnormal neuronal phenotype in cortical neurons derived from autism-associated *Shank3* patients.

METHODS:

iPSC culture and generation of cortical Neural Progenitor cells (NPCs)

iPSCs carrying a (c.3679insG) *Shank3* mutation and the control iPSCs were previously[13] generated from a female child and its unaffected mother's fibroblasts respectively. iPSCs were cultured and maintained using mTesR PLUS media. Cortical neurons were generated using a previously described protocol [14,27,28]. In brief, iPSCs were grown to ~80% confluency, then dissociated using Dispase (StemCell Technologies, Cat #07923) and plated onto low-adherence plates (Falcon, 351007) in mTeSR medium with ROCK inhibitor, allowing for the formation of embryonic bodies (EBs). The media was changed on the next day to mTeSR PLUS without ROCK inhibitor. In the following 10 days, the cells were fed with EB media containing: DMEM/F12 with Glutamax (1:100, Gibco, Cat #35050038), B27 with Retinoic Acid (1:100,

Gibco, Cat #17504044), N2 supplement (1:100, Gibco, Cat #17502048), and 0.1uM LDN193189 Hydrochloride (Biogems, Cat #1066208). The EBs were plated onto poly-L-ornithine/laminin (Sigma-Aldrich, Cat # P3655, R&D Systems, Cat #3400-010-03) coated six-well dishes in DMEM/F12 plus N2, B27, and laminin for the following 7 days to allow the formation of neural rosettes. The rosettes were selected based on their morphology and were manually picked, dissociated (with Accutase (StemCell Technologies, Cat #07920)) and plated onto poly-l-ornithine/laminin-coated plates in neural progenitor cell (NPC) medium containing: DMEM/F12 with Glutamax (1:100), B27 supplement with RA 50X (1:50), N2 supplement 100X (1:100), laminin (1 mg/ml), and 20 ng/ml bFGF. Full media change was performed every second day for the following 7-12 days until full confluency.

Differentiation of cortical NPCs into cortical neurons

Cortical NPCs were differentiated into cortical neurons by a differentiation medium containing: DMEM/F12, N2, B27, Glutamax, 200 picoMol L-Ascorbic Acid (Biogems, Cat #5088177), 500 µg/ml Dibutyryl-cAMP (Adooq, Cat #A15914-5), 1 mg/ml laminin, 20 ng/ ml Brain-derived neurotrophic factor (BDNF) (Peprotech, Cat #AF-450-02) (20 ng/ ml), and 20 ng/ml Glial cell line-derived neurotrophic factor (GDNF)(Peprotech, Cat # 450-10) for 10 days. Between days 11 and 14, the cells were dissociated again and then fed with Brainphys medium with B27, N2, L-ascorbic acid (200 picoMol), cyclic AMP (500 µg/ml), BDNF (20 ng/ml), GDNF (20 ng/ml), and laminin (1 mg/ml). The neurons were differentiated for up to 5 weeks and the experiments were performed starting 4 weeks of differentiation.

Exosome Isolation and treatment

Exosomes from Control and Shank3 neurons

The exosomes were purified from iPSC-derived Control and *Shank3* cortical neurons using differential centrifugation followed by an ultra-centrifugation method as described previously [29]. Briefly, the iPSC-derived cortical neurons were cultured and maintained in cortical neuronal differentiation media as described above devoid of any exogenous source of exosomes. The

culture media collected from the iPSC-derived cortical neurons were centrifuged for 10 min. at 300*g* at 4 °C. The pellet was discarded and the supernatant was recovered and re-centrifuged for 10 min. at 2000*g at* 4 °C. The pellet of dead cells was then discarded and the supernatant was collected again and centrifuged for 30 min. at 10,000*g* (4 °C) to remove the cell debris. The supernatant (free of dead cells and cell debris) was filtered through a 0.22-µm filter and ultra-centrifuged for 70 min at 100,000*g* (4 °C). The pellet containing the exosomes and proteins was washed in 0.22-µm filtered PBS and then ultra-centrifuged again for 70 min. at 100,000*g* (*4 °C*). Finally, the pellet containing the purified exosomes was re-suspended in 100-200 µl of filtered and sterilized PBS. Exosomes from control and *Shank3* cortical neurons were switched two times –one during the first 7 days of differentiation and the second approximately 14-15 days of differentiation

Exosomes from MSCs and iPSCs

Human bone marrow MSCs (Lonza, Cat #PT-2501) were cultured in DMEM/F12 medium, supplemented with 1% 200mM L-glutamine(Thermo Scientific, Cat # 25030081), 1% MEM-Eagle nonessential amino acid (Thermo scientific Cat # 11140050), 0.04% heparin(Sigma, Cat # H3393), and 10% exosome-free platelets lysate (Rabin Medical Center, Israel) for 3 days. Conditioned media was collected from the cells and exosome isolation was done using a differential centrifugation method followed by ultracentrifugation as described previously[29,30]. For, iPSC-exo, iPSCs from a healthy individual were cultured as described above and the exosomes were isolated by the same process described above after the collection of the spent media from the culture of control healthy iPSCs.

Exosomes from MSCs and iPSCs were applied three times on *Shank3* cortical neurons. First within 3-4 days of differentiation, second after 14-15 days of differentiation, and third after 23-24 days of differentiation. The electrophysiology was performed within a week of the last treatment of exosomes approximately 29-30 days of differentiation.

Synthetic liposomes production

Synthetic liposomes were produced as described previously[31] using a Nanoassemblr (Precision nanosystem). Synthetic liposome treatment was performed two times at a similar time point as the exosome switching experiment.

Exosome characterization, labeling, and uptake

Exosomes were characterized using Zetasizer (Malvern Panalytical) for charge, particle size, and concentration using dynamic light scattering (DLS) and electrophoretic light scattering methods (ELS). Briefly, for size and concentration, 10 ul of exosomes were diluted in 990 ul of 0.22 µm filtered PBS (1X) in disposable size cuvettes (DTS0012) and measurements were done using Ultra-pro ZS Xplorer software. For charge, 10 ul of exosomes were diluted in 90 ul of PBS (1X) and 900 ul of MilliQ water in a glass ZP cuvette (DTS1070). The measurements were done similarly in size and concentration between all the samples. Further, the exosomes were characterized using proteomics for the protein markers as described below. Exosomes were labeled using PKH-67 (Merck, MIDI67) dyes as described previously [30,32]. For labelling and treatment the cortical neurons were incubated with 2-3*10^{10} particles. The labelled exosomes were imaged within 24 hours of incubation, and were clearly observed to be up taken by the neurons.

Electrophysiology

Whole-cell patch-clamp recordings were performed in SHANK3 mutant cortical neurons, and from control neurons that were treated with exosomes isolated from neurons, MSCs, and iPSCs based on previously described methods[33,34] 4-5 weeks after the start of the differentiation. Culture coverslips were placed inside a recording chamber filled with HEPES-based artificial cerebrospinal fluid (ACSF) containing (in mM): 10 HEPES (Sigma-Aldrich, Cat #H0887-100ML), 139 NaCl (Sigma-Aldrich, Cat #S9888), 4 KCl (Sigma-Aldrich, Cat #P3911), 2 CaCl2 (Sigma-Aldrich, Cat #223506), 10 D-glucose (Sigma-Aldrich, Cat # G7021), and 1MgCl2 (Merck, Cat #7791-18-6) (pH 7.5, osmolarity was adjusted to 310 mm). Fire-polished borosilicate glass capillaries (Sutter Instrument, Cat #BF150-75-10) were pulled (tip resistance

of about 9–12 MΩ) using a (P1000, Sutter Instrument, Novato, CA, United States) and filled with an internal solution containing (in mM): 130 K-gluconate, 6 KCl, 4 NaCl, 10 Na-HEPES, 0.2 K-EGTA, 0.3 GTP, 2 Mg-ATP, 0.2 cAMP, 10 D-glucose, 0.15% biocytin and 0.06% rhodamine (pH 7.5, osmolarity adjusted to 290–300 mOsm). All measurements were done at room temperature using a patch clamp amplifier (MultiClamp 700B, Molecular Devices, San Jose, CA, United States), connected to a digitizer (Axon Digidata 1550B, Molecular Devices, San Jose, CA, United States), and controlled by MultiClamp 700B Commander and pCLAMP 11 software. Data were acquired at a sampling rate of 20 kHz and analyzed using Clampfit-10 and the software package MATLAB (release 2014b; The MathWorks, Natick, MA, USA).

Analysis of electrophysiological recordings

The acquired data was analyzed based on previously described methods [33] using custom-written MATLAB scripts. Briefly:

(a) Sodium, fast, and slow potassium currents. Neurons were held in voltage clamp mode at −60 mV, and voltage steps of 400 ms were performed in the −100 to 90 mV range. Currents were typically normalized by the cells' capacitance. The sodium (Na+) current was computed by subtracting the sodium current after stabilization from the lowest value of the inward sodium current. The fast potassium (K+) currents were measured by the maximum outward currents that appeared within a few milliseconds after a depolarization step. The slow K+ currents were measured at the end of the 400 ms depolarization step. A one-way ANOVA test was performed for the statistical analysis between the groups.

(b) Synaptic currents analysis. The mean and standard error (SE) of the excitatory postsynaptic currents (EPSCs) amplitudes for each active cell were calculated. The cumulative distribution of EPSC amplitude was calculated for each group and condition. The frequency of the events for each cell was calculated by dividing the number of events by the duration of the recording (non-active cells were included with an event rate of 0 Hz). The mean rates and standard errors

of EPSC frequencies of all the cells in each group were computed. Non-parametric statistical tests (Mann-Whitney U test) were performed for comparisons.

(c) *Evoked action potentials* (APs). Neurons were held in current clamp mode at −60 mV with a constant holding current. Following this, current injections were given in 3 pA steps with 400 ms duration, starting 12 pA below the steady-hold current. A total of 38 depolarization steps were given. The total evoked action potential was the total number of action potentials that were counted in the 38 depolarization steps. Non-parametric statistical tests (Mann-Whitney U test) were performed for comparisons between the groups since the data were not normally distributed.

Proteomics

For Proteomics, The LC-MS/MS facility at the *Smoler Proteomics Centre* facility at Technion, Haifa, Israel was availed. Briefly, the exosomes ~50 ul (10^{14}- 10^{15} particles/ul) were lysed in RIPA buffer and the exosome-RIPA buffer mix was then incubated on ice for 20-30 mins for the extraction of proteins. The sample was then centrifuged at 16000g for 10 min. at 4 °C. The cleared lysate (supernatant) was used for protein estimation using the Pierce ™ (BCA) assay kit (Thermo Scientific, 23225). The extracted protein was trypsinized and the samples were subjected to the LC-MS/MS analysis using the Q Exactive HF mass spectrometer. The data was analyzed using the Proteome Discoverer 2.4 software. The graphs for proteomics data analysis were made using the Funrich analysis tool [35,36]. The volcano plots for differentially expressed proteins between different exosomes were plotted using MATLAB [37].

Immunocytochemistry (ICC)

Cells on coverslips were fixed in 4% paraformaldehyde for 15 min. and then washed 3 times with DPBS for 5 min. in each step, blocked, and permeabilized in PBS containing 0.1–0.2% Triton X-100 and 10% horse serum. Next, the coverslips were incubated with primary antibodies; for Neurons: chicken anti-MAP2 (Abcam, ab92434, 1:500), rabbit anti-TBR1 (Abcam, ab183032, 1:250), rabbit anti-VGLUT1 (Abcam, ab227805, 1:500) and Mouse anti-

GABA (Abcam, ab86186, 1:400) in the blocking solution overnight at 4 °C. On the next day, the coverslips were washed in DPBS and incubated with DAPI (Abcam, ab228549, 1:1000) and the corresponding secondary antibodies for 60 min. at room temperature. Then, the coverslips were washed three times, mounted on glass slides using Fluromount-G (mounting medium), and dried overnight while being protected from the light. Microscopy was performed using a Leica THUNDER imager and an Olympus Confocal microscope. The images were analyzed using ImageJ and MATLAB.

RESULTS:

Cortical neuron differentiation from Control and *Shank3* (c3679insG) iPSC lines

Shank3 is ~190 kDa protein with a multi-domain architecture including an SH3 domain, a proline-rich domain, a PDZ domain, and ankyrin repeat domains[35]. The c3679insG mutation of *Shank3* has been previously characterized in the transgenic mice model and is located in the Exon-21 of *Shank3* (Proline-rich domain)[12](Fig.1a,b). Single-cell RNA sequencing data available from the UCSC browser reveals that *Shank3* is abundantly expressed in the cortex and cerebellum region of the human fetal & adult brain; comparatively more in excitatory and subtypes of inhibitory neurons than astrocytes, oligodendrocytes, and microglial cells (Fig. 1c).

We have recently generated iPSC lines with *Shank3* c3679insG mutation from a patient and a first-degree relative[13]. We further differentiated these iPSC lines into cortical NPCs and neurons (Fig. 1d) (see methods). We isolated exosomes from control and *Shank3* cortical neurons by ultracentrifugation (see methods) and characterized the size and zeta potential by dynamic light scattering (Fig 1e & f). The size of control neurons exosomes was approximately 101.8±31.35 nm and the shank3 neurons exosomes size was 66.14±33.9 nm. Control neurons' exosomes had an average zeta potential of -8.6±2.44 mV while the *Shank3* neuron exosomes had an average zeta potential of -5.7±0.45 mV. We next labeled the isolated exosomes using the PKH-67 dye and verified the uptake of exosomes in control cortical neurons (Fig 1g).

Exosomes from *Shank3* neurons induce *Shank3* phenotypes in control neurons

As previously reported, cortical neurons from *Shank3* mutant lines exhibited an accelerated maturation with early hyper-excitability, increased Na+/K+ currents, and increased rate of excitatory postsynaptic currents (EPSCs) compared to control neurons when the neurons were differentiated for 4-5 weeks [14]. We performed the switching of exosomes two times between control and *Shank3* neurons and measured the effect on the electrophysiological characteristics of the cells (Fig 2a); i.e. the control cortical neurons were treated with exosomes isolated from *Shank3* neurons and vice-versa. We further performed immunostaining with neuronal marker MAP2 and cortical neuronal markers TBR1 and CTIP2 for untreated control neurons and exosome-treated neurons (Fig 2b). The ICC shows a high expression percentage of cortical markers in the differentiated neuronal culture (both treated and untreated) (Supplementary Fig. 1).

After exosome switching, we performed a patch-clamp when the neurons were in the fifth week of *in-vitro* differentiation for treated and untreated control neurons (Fig 2). The control cortical neurons displayed normal Na+/K+ currents like young cortical neurons (Fig 2c). Comparatively, although not statistically significant, the *Shank3* exosome-treated Control neurons showed a trend toward increased Na+ currents after exosome swapping. (Fig 2d,f). The slow and fast K+ currents were unchanged after *Shank3* exosome treatment in control neurons (Fig 2g,h). We also included a treatment with synthetic liposomes of ~100 nm size (see methods) to determine if that would also have a similar effect as *Shank3* exosomes on control cortical neurons (Fig 2e). We found that synthetic liposome treatment had the opposite effect causing a decrease in Na+/K+ currents in control cortical neurons (Fig 2f-h).

We then measured the evoked action potential (AP) after the current injection at the current clamp mode. The representative traces of the total evoked APs for control cortical neurons and control neurons treated with *Shank3* exosome have been plotted in (Fig 2i-k). Surprisingly, the *Shank3* exosome-treated control neuron displayed increased total evoked APsand were hyper-excitable compared to the Control cortical neurons in the same time point (Fig 2l). The synthetic liposome treatment to control cortical neurons, however, caused a decrease in total evoked APs

and hence the excitability. (Fig 2l). Next, we investigated the total spontaneous action potential (APs) or firing rate of neurons in the absence of any external current stimulus holding the cell at -45 mV. The representative traces of the total spontaneous APs in control neurons and shank3 mutant neurons have been plotted in Fig 2(m-o). Similar to the total evoked APs, the spontaneous APs were higher in *Shank3* exosome-treated control neurons compared to the untreated control neurons (Fig 2p). The synthetic liposome treatment on control cortical neurons decreased the spontaneous APs and hence had a contrasting effect compared to *Shank3* neuron exosomes (Fig 2o,p).

We further measured the AMPA receptor-mediated excitatory postsynaptic current (EPSC) events at voltage-clamp mode (see methods) to analyze the synaptic activity of the control neuron at the fifth week of cortical differentiation. The representative traces of EPSCs rate and amplitudes for control, *Shank3-derived* exosomes, and synthetic liposomes treated control neurons have been plotted in Fig 2q-s. However, contrary to the total evoked APs, in the *Shank3* exosome-treated control neurons the EPSC rate was not altered and remained similar to control cortical neurons (Fig 2t). In addition, the EPSC amplitude analysis also did not find any significant change among the three groups (Fig 2u).

Shank3 **cortical neurons maintain accelerated maturation and hyperexcitability phenotype after treatment with control neuron-derived exosomes**

Similarly, we measured and analyzed the electrophysiological properties of *Shank3* neurons after exosome switching. The immunostaining performed on *Shank3* neurons and control exosomes treated Shank3 neurons showed high expression of cortical markers (TBR1 and CTIP2) along with neuronal MAP2 (Fig 3a & Supplementary Fig. 2a)). As mentioned above, *Shank3* displayed increased normalized Na+/K+ currents (Fig 3b-c), as shown in representative traces, reminiscent of mature membrane properties at relatively younger ages than control neurons (Fig 2c-d). The Control exosome-treated *Shank3* neurons had similar Na+/K+ currents as untreated *Shank3* neurons (Fig 3d-f).

The evoked action potential (AP) measured after the current injection at the current clamp mode showed an increased number of spikes per depolarisation step as well as the total number of spikes was higher for *Shank3* neurons compared to control neurons (Fig 3g-i). However, control exosome treatment did not alter the hyperexcitability of *Shank3* neurons.

Similarly, we recorded the total spontaneous APs by holding the cells at -45 mV and without external current injection. The spontaneous APs were high in *Shank3* neurons similar to total evoked potential as seen in Fig 3 (j,k) respectively. Notably, control exosome treatment did not change the spontaneous APs firing rate of the *Shank3* neurons (Fig 3l). The AMPA receptor-mediated EPSC rate and amplitude were also significantly higher in *Shank3* mutant neurons compared to the control neurons (Fig 3m-o, Fig2t;) as also previously reported[14] (Fig2u; Fig 3p). *Shank3* neurons maintained the high EPSC rate and amplitude even after treatment with control exosomes during exosome switching (Fig 3o,p).

Hence, these results (Figs 2 and 3 collectively) provide evidence that treatment with exosomes from *Shank3* neurons can significantly influence the neurophysiology of Control cortical neurons and make them hyper-excitable, whereas treatment with control exosomes to *Shank3* neurons possesses no substantial effect.

Mesenchymal stem-cell-derived exosomes rescue *Shank3* cortical neuronal phenotypes

Mesenchymal stem cell (MSC) derived exosomes (MSC-exo) have been previously shown to have rescued behavioral deficits in mouse models of Autism[32] and Schizophrenia[38]. Hence, we wanted to examine if MSC-exo can rescue the neurophysiological deficits of human Shank3 mutant cortical neurons. We isolated exosomes from MSCs (see methods) and treated *Shank3* mutant neurons (see methods) (Fig 4a,b) with purified MSC-exo (approx. $2*10^{10}$ exosome particles per $2.5*10^{5}$ cells/well), and measured the electrophysiological properties of the treated neurons using whole cell patch clamp. The average size of MSC exosomes was 80.26±14.37 nm and the zeta potential was -16.7(±1.34) mV. Immunostaining was performed for MAP2,

TBR1, and CTIP2 in the untreated and MSC-exo-treated *Shank3* mutant neurons (Fig 4c& Supplementary Fig. 2b). The ICC shows a high expression of cortical markers in the differentiated neuronal culture (both treated and untreated).

Fig 4(d-e) shows representative traces for the normalized Na+/K+ currents (at voltage-clamp mode) of *Shank3* mutant cortical neurons with and without MSC-exo treatment at 4-5 weeks of *in-vitro* differentiation. MSC-exo treatment of *Shank3* mutant neurons significantly reduced the Na+ and K+ currents of the *Shank3* neuron by 1.5 fold (Fig 4f-h) compared to untreated Shank3 mutant neurons. The total number of evoked APs (in current-clamp mode) also showed approximately a two-fold reduction in the excitability of *Shank3* mutant neurons (Fig 4i-k) compared to untreated mutant neurons. Additionally, the total number of spontaneous APs (see methods) showed a decreasing trend in the number of APs (p=0.29) after MSC-exo treatment compared to untreated neurons (Fig 4i-n for representative images and averages).

We then analyzed EPSCs in voltage-clamp mode and found a significant reduction in the EPSC rate and amplitude in the MSC-exo treated *Shank3* neuron (hold at -60mV) compared to untreated *Shank3* cortical neurons (Fig 4o-r). These results show that exosomes isolated from MSCs rescue most of *Shank3* mutant cortical neuron phenotypes.

iPSC-derived exosomes rescue *Shank3* cortical neuronal phenotypes

Subsequently, we aimed to examine if exosomes derived from control iPSCs (iPSC-exo) could also rescue the phenotypes of *Shank3* cortical neurons compared to untreated neurons (Fig 5a). Hence, we isolated exosomes from the iPSC culture medium and treated the *Shank3* mutant neurons with approx. 2- $4*10^{10}$ exosome particles per $2.5*10^{5}$ cells/well, and measured the neurophysiological properties using a whole cell patch clamp (Fig 5a,b). The average size of the isolated exosomes was 87.82±34.54 nm and the zeta potential was -20.7(±1.02) respectively. Fig 5c shows immunostaining for *Shank3* mutant neurons with MAP2, TBR1, and CTIP2 antibodies in untreated and treated neurons (also see Supplementary Fig. 2c).

The normalized Na+ and K+ currents of *Shank3* neurons were significantly reduced after iPSC-exo treatment compared to untreated neurons measured in voltage-clamp mode as shown in representative traces and average plots (Fig 5d-h). The total number of evoked APs (measured in current clamp mode, see methods) also demonstrated a reduction in the hyper-excitability phenotype in *Shank3* mutant neurons after iPSC-exo treatment compared to untreated neurons shown in representative traces and average plots (Fig 5i-k). Similarly, the total spontaneous APs (see methods) were decreased in the treated neurons compared to non-treated neurons (representative and average plots are shown in Fig 5l-n).

Finally, we measured the EPSC rate and amplitude (in voltage clamp mode, see methods) in the iPSC-exo-treated *Shank3* mutant neurons compared to untreated shank3 mutant neurons which were reduced but not significantly (p=0.0617) after iPSC-exo treatment (Fig 5o-r). Overall, our results show that exosomes derived from iPSCs rescue most neurophysiological phenotypes in *Shank3* mutant neurons.

Proteomic analysis of exosomes

To better understand how the different exosomes affect the neurophysiology of neurons, we performed quantitative proteomics using LC-MS/MS to identify the protein cargoes of the four types of exosomes that we isolated for the treatment of control and *Shank3* mutant neurons. These included – Control neurons' exosomes, *Shank3* mutant neurons' exosomes, MSC, and iPSC exosomes. We detected a larger number of proteins in *Shank3* neuron exosomes (216 proteins) and MSC–exo (217 proteins) as compared to Control neuron exosomes (114 proteins) and iPSC-exo (32 proteins) (Fig 6a presents the number of common proteins between the different exosomes). A cellular component analysis of protein cargoes from all four cell sources showed significant enrichment for "exosomes" and "extracellular " proteins ($p<0.001$, Fig 6b). Additionally, the neuron-derived exosomes also showed enrichment for "cytoplasm" ($p<0.001$) but not the stem cell-derived exosomes.

The differential protein expression analysis between the four groups is plotted in Fig. 6 (c,e,g, i) & Supplementary Fig. 3 as volcano plots. The biological pathways analysis of the protein cargoes for the corresponding volcano plots is presented in Fig 6 (d,f,h,j). "Cell adhesion", "Cell growth/ or maintenance", "Protein metabolism", and "Apoptosis" were among the highly enriched biological pathways in *Shank3* mutant neurons' exosomes compared to exosomes derived from control neurons. "Chromosome organization and biogenesis", "Peptide metabolism", Protein folding, "Cell proliferation" and "regulation of cell cycle" were depleted in *Shank3* mutant exosomes compared to control neuron exosomes (Fig 6d.). When comparing proteins extracted from MSCs and iPSCs compared to control neurons' exosomes, "Chromosome organization and biogenesis", "Peptide metabolism", "Protein folding", and "Cell proliferation" were commonly enriched (Fig 6d.f,h). Further, when comparing MSC-exo and iPSC-exo protein cargoes, we found "Regulation of cell cycle", "Cell cycle", "Anti-apoptosis", "Complement activation", and "Cell adhesion" to be enriched while "Apoptosis", "Transport", "Cell growth/ or maintenance", "Signal transduction" to be down-regulated (Fig 6d.j).

DISCUSSION:

The absence of distinct pathological hallmarks in ASD has been a limiting factor in detecting possible effects of therapeutic drugs and molecules, due to the lack of suitable read-out modalities. ASD, unlike several neurodegenerative diseases, such as AD and PD, does not exhibit protein aggregation pathologies like Amyloid-beta plaques or *Lewy bodies* in neurons that can serve as biomarkers and targets for novel therapeutics. Our current study along with previous studies has identified the accelerated maturation in iPSC-derived neurons of individuals with ASD with *Shank3* and other ASD-associated mutations as one potential endophenotype and read-out[14,39–41]. This accelerated maturation was measured by increased Na+/K+ currents, increased excitability, and increased EPSC rate early in the differentiation

[14,42]; as well as in transcriptomic and morphological analysis [39]. Further, evidence for increased neuronal connections at the early stages of the development was observed in an fMRI study of children with ASD that found brain hyperconnectivity correlated with the severity of social dysfunction [43]. Additionally, increased spine density was found in the post-mortem brain samples of children with ASD in the age of 2-9 years compared to age-matched controls[44,45]. These findings point to increased synaptic connections in ASD and thereby correlate to the increased EPSC frequency that we have observed in patients' iPSC-derived neurons from *Shank3* and other ASD-associated genes.

Exosomes hold great potential in translational research especially in therapeutics and diagnostics due to their role in inter-cellular communication [18]. We started the study by switching the exosomes isolated from healthy and *Shank3* mutant neurons. Surprisingly, treating control neurons with exosomes derived from *Shank3* mutant neurons was sufficient to induce ASD phenotypes in the control neurons. However, the exosomes derived from control neurons did not rescue the phenotypes of *Shank3* mutant neurons. Recent studies have demonstrated that the source or parent cells from which the exosomes are produced greatly influence the cargo they carry to the recipient cells [17,46,47]. Our results have thus important implications for understanding the pathophysiology of ASD as well as cellular communications mediated via exosomes in the human central nervous system. We demonstrate the effect of exosomes isolated from different cells on neuronal function and connectivity. Interestingly, in this study, we show for the first time that exosomes derived from MSCs and iPSCs rescue abnormal neurophysiological phenotypes of *Shank3* mutant neurons, and also these phenotypes can be transferred to control neurons via exosomes derived from the mutant neurons. The trans-synaptic mode of communication via exosomes has been demonstrated previously for proteins and cell-signaling factors in the neuromuscular junction in *Drosophila* [48,49]. Hence, the transfer of intrinsic properties of excitability of ASD neurons through our results further reinforces an alternative mode of communication between human neuronal cells via exosomes.

Despite the clear genetic basis of *Shank3*-related pathologies, there are currently no approved drugs specifically targeting the broader spectrum of core ASD symptoms in patients with *Shank3* mutations. Given the ability of stem-cell-derived exosomes to cross the blood-brain barrier and being minimally invasive[50], they offer hope as a possible therapeutic approach for neurological disorders[26]. We tested the effects of purified exosomes from MSCs and iPSCs on *Shank3* cortical neurons to better understand their impact on neuronal intrinsic properties and synaptic connections. Some beneficial properties of MSCs have been attributed to their paracrine effect mediated via extracellular vesicles[51]. Exosomes derived from MSCs, similar to the MSCs, possess anti-inflammatory, immunomodulatory, and neuroprotective effects[24]. In our study, we found that MSC-derived exosomes rescue the accelerated maturation of *Shank3* mutant neurons. Notably, MSC-derived exosomes were previously shown to rescue social interaction and communication deficits in mouse models of autism [30,32].

Although MSC-derived exosomes have shown promise for clinical applications, certain limitations in scaling up MSC cultures for exosome production present significant challenges[52]. MSCs, for example, have a limited proliferative capacity and have been found to exhibit chromosome variability, cellular senescence, and molecular changes after 4-5 passages in *in vitro* cultures leading to higher costs for exosome production[53,54]. In addition, to extract MSCs, a donor needs to undergo an invasive procedure. Furthermore, the donor source and isolation methods can affect the quality and potency of MSCs and thus the exosomes produced from them[55]. Due to their pluripotent nature, iPSCs offer solutions to these challenges with their almost unlimited proliferative capacity, comparatively lesser chromosomal variability, and higher consistency in *in vitro* conditions facilitating large-scale production for therapeutic use[56,57]. iPSCs can be produced with minimal stress to the donor (a blood or even a urine sample). Similar to MSC-derived exosomes, we found that iPSC-derived exo rescued the accelerated maturation in *Shank3* mutant neurons.

Proteomic analysis of exosomes derived from *Shank3* mutant and control neurons, as well as from MSC- iPSC derived exosomes, revealed distinct protein cargo profiles, especially

differences were observed between exosomes derived from stem cells (MSCs and iPSCs) and exosomes derived from neurons (control and shank3 mutant). Importantly, although MSC-derived exosomes and iPSC-derived exosomes had similar protective effects on the *Shank3* mutant neurons, the protein cargo was not identical with more than half of the unique protein content. The MSCs are multipotent and mesodermal in nature while iPSCs can differentiate into the three germ layers. Hence, the proteomic profile of the exosomes likely reflects the underlying physiological properties of the parent cells[46]. Interestingly, we also found that MSC-derived exosomes carry a larger protein cargo load compared to iPSC–derived exosomes. However, towards the development of exosome-based therapies, we believe it would be more practical to engineer exosomes with minimal cargo while maintaining comparable efficacy to those with a larger cargo load given the complexity of intermolecular interactions.

In conclusion, using accelerated maturation as an endophenotype for ASD-associated mutations, we provide evidence that exosomes can change the intrinsic and network properties of *Shank3* mutant neurons as well as offer a potential therapeutic approach for modulating neuronal function in neurodevelopmental disorders. The ability of exosomes to transfer pathological phenotypes between neurons reinforces their significance in intercellular communication and highlights the need for further research into their therapeutic applications. Future studies should focus on characterizing the specific cargo carried by exosomes from different cell types and understanding the molecular mechanisms through which they influence the recipient cells. This will be essential for developing targeted exosome-based therapies for ASD and related neuropsychiatric disorders.

DATA AVAILABILITY

The data that supports the findings of this study are available upon reasonable request from the authors.

CODE AVAILABILITY

The MATLAB codes used for electrophysiology data analysis and figure generation are available upon reasonable request from the authors.

ACKNOWLEDGMENTS

The Zuckerman STEM leadership program and Israel Science Foundation grants - 1994/21 and 3252 /21 for Dr. Shani Stern. The schematic images in the manuscript were drawn using Biorender.com.

ETHICS DECLARATION

Competing Interests

The Authors declare no competing financial or non-financial Interests.

AUTHOR CONTRIBUTION:

AC and **IR** (co-first authors) contributed equally to the work**. AC**- Experiments-Cell culture, Exosome isolation, labeling, quantification, Immunocytochemistry, Proteomics Data Analysis, Methodology design, Drafting the original manuscript. **IR-** Electrophysiology, Exosome quantification, help in drafting the original manuscript, Methodology design. **YH-** Electrophysiology Data analysis. **AS-** Proteomics Data analysis. **WAR-** cell culture experiments. **DO**-Resource availability for exosomes. **AZ**-Resource availability for exosome quantification. **SS** (corresponding author)- Supervision, Conceptualization, Methodology design, MATLAB codes for Data Analysis, Editing –original manuscript. All authors reviewed the manuscript.

REFERENCES:

1. Du, Y., Weed, S.A., Xiong, W.-C., Marshall, T.D., and Parsons, J.T. (1998). Identification of a Novel Cortactin SH3 Domain-Binding Protein and Its Localization to Growth Cones of Cultured Neurons. Molecular and Cellular Biology *18*, 5838–5851. https://doi.org/10.1128/MCB.18.10.5838.

2. Naisbitt, S., Kim, E., Tu, J.C., Xiao, B., Sala, C., Valtschanoff, J., Weinberg, R.J., Worley, P.F., and Sheng, M. (1999). Shank, a novel family of postsynaptic density proteins that binds to the NMDA receptor/PSD-95/GKAP complex and cortactin. Neuron *23*, 569–582. https://doi.org/10.1016/s0896-6273(00)80809-0.

3. Woelfle, S., Pedro, M.T., Wagner, J., Schön, M., and Boeckers, T.M. (2023). Expression profiles of the autism-related SHANK proteins in the human brain. BMC Biology *21*, 254. https://doi.org/10.1186/s12915-023-01712-0.

4. Grabrucker, A.M., Schmeisser, M.J., Schoen, M., and Boeckers, T.M. (2011). Postsynaptic ProSAP/Shank scaffolds in the cross-hair of synaptopathies. Trends in Cell Biology *21*, 594–603. https://doi.org/10.1016/j.tcb.2011.07.003.

5. Anderlid, B.-M., Schoumans, J., Annerén, G., Tapia-Paez, I., Dumanski, J., Blennow, E., and Nordenskjöld, M. (2002). FISH-mapping of a 100-kb terminal 22q13 deletion. Human Genetics *110*, 439–443. https://doi.org/10.1007/s00439-002-0713-7.

6. Wilson, H.L., Wong, A.C.C., Shaw, S.R., Tse, W.-Y., Stapleton, G.A., Phelan, M.C., Hu, S., Marshall, J., and McDermid, H.E. (2003). Molecular characterisation of the 22q13 deletion syndrome supports the role of haploinsufficiency of SHANK3/PROSAP2 in the major neurological symptoms. J Med Genet *40*, 575–584. https://doi.org/10.1136/jmg.40.8.575.

7. Costales, J.L., and Kolevzon, A. (2015). Phelan–McDermid Syndrome and SHANK3: Implications for Treatment. Neurotherapeutics *12*, 620–630. https://doi.org/10.1007/s13311-015-0352-z.

8. Reim, D., Distler, U., Halbedl, S., Verpelli, C., Sala, C., Bockmann, J., Tenzer, S., Boeckers, T.M., and Schmeisser, M.J. (2017). Proteomic Analysis of Post-synaptic Density Fractions from Shank3 Mutant Mice Reveals Brain Region Specific Changes Relevant to Autism Spectrum Disorder. Frontiers in Molecular Neuroscience *10*.

9. Gauthier, J., Champagne, N., Lafrenière, R.G., Xiong, L., Spiegelman, D., Brustein, E., Lapointe, M., Peng, H., Côté, M., Noreau, A., et al. (2010). De novo mutations in the gene encoding the synaptic scaffolding protein SHANK3 in patients ascertained for schizophrenia. Proceedings of the National Academy of Sciences *107*, 7863–7868. https://doi.org/10.1073/pnas.0906232107.

10. Moessner, R., Marshall, C.R., Sutcliffe, J.S., Skaug, J., Pinto, D., Vincent, J., Zwaigenbaum, L., Fernandez, B., Roberts, W., Szatmari, P., et al. (2007). Contribution of SHANK3 Mutations to Autism Spectrum Disorder. The American Journal of Human Genetics *81*, 1289–1297. https://doi.org/10.1086/522590.

11. Huang, C., Voglewede, M.M., Ozsen, E.N., Wang, H., and Zhang, H. (2023). SHANK3 Mutations Associated with Autism and Schizophrenia Lead to Shared and Distinct Changes in Dendritic Spine Dynamics in the Developing Mouse Brain. Neuroscience *528*, 1–11. https://doi.org/10.1016/j.neuroscience.2023.07.024.

12. Zhou, Y., Kaiser, T., Monteiro, P., Zhang, X., Van der Goes, Marie.S., Wang, D., Barak, B., Zeng, M., Li, C., Lu, C., et al. (2016). Mice with Shank3 Mutations Associated with ASD and Schizophrenia Display Both Shared and Distinct Defects. Neuron *89*, 147–162. https://doi.org/10.1016/j.neuron.2015.11.023.

13. Nayak, R., Rosh, I., Rabinski, T., Falik, D., Mendel Percia, M., and Stern, S. (2022). Generation and characterization of iPSC lines (UOHi003-A, UOHi002-A) from a patient with SHANK3 mutation and her healthy mother. Stem Cell Res *64*, 102899. https://doi.org/10.1016/j.scr.2022.102899.

14. Hussein, Y., Tripathi, U., Choudhary, A., Nayak, R., Peles, D., Rosh, I., Rabinski, T., Djamus, J., Vatine, G.D., Spiegel, R., et al. (2023). Early maturation and hyperexcitability is a shared phenotype of cortical neurons derived from different ASD-associated mutations. Translational Psychiatry *13*, 246. https://doi.org/10.1038/s41398-023-02535-x.

15. Yi, F., Danko, T., Botelho, S.C., Patzke, C., Pak, C., Wernig, M., and Südhof, T.C. (2016). Autism-associated SHANK3 haploinsufficiency causes Ih channelopathy in human neurons. Science *352*, aaf2669. https://doi.org/10.1126/science.aaf2669.

16. Peixoto, R.T., Wang, W., Croney, D.M., Kozorovitskiy, Y., and Sabatini, B.L. (2016). Early hyperactivity and precocious maturation of corticostriatal circuits in Shank3B−/− mice. Nature Neuroscience *19*, 716–724. https://doi.org/10.1038/nn.4260.

17. Miron, R.J., and Zhang, Y. (2024). Understanding exosomes: Part 1—Characterization, quantification and isolation techniques. Periodontology 2000 *94*, 231–256. https://doi.org/10.1111/prd.12520.

18. Kalluri, R., and LeBleu, V.S. (2020). The biology, function, and biomedical applications of exosomes. Science *367*. https://doi.org/10.1126/science.aau6977.

19. Zou, J., Peng, H., and Liu, Y. (2021). The Roles of Exosomes in Immunoregulation and Autoimmune Thyroid Diseases. Front Immunol *12*, 757674. https://doi.org/10.3389/fimmu.2021.757674.

20. Soria, F.N., Pampliega, O., Bourdenx, M., Meissner, W.G., Bezard, E., and Dehay, B. (2017). Exosomes, an Unmasked Culprit in Neurodegenerative Diseases. Front Neurosci *11*, 26. https://doi.org/10.3389/fnins.2017.00026.

21. Frühbeis, C., Fröhlich, D., Kuo, W.P., Amphornrat, J., Thilemann, S., Saab, A.S., Kirchhoff, F., Möbius, W., Goebbels, S., Nave, K.-A., et al. (2013). Neurotransmitter-Triggered Transfer of Exosomes Mediates Oligodendrocyte–Neuron Communication. PLOS Biology *11*, e1001604. https://doi.org/10.1371/journal.pbio.1001604.

22. Fröhlich, D., Kuo, W.P., Frühbeis, C., Sun, J.-J., Zehendner, C.M., Luhmann, H.J., Pinto, S., Toedling, J., Trotter, J., and Krämer-Albers, E.-M. (2014). Multifaceted effects of oligodendroglial exosomes on neurons: impact on neuronal firing rate, signal transduction and gene regulation. Philosophical Transactions of the Royal Society B: Biological Sciences *369*, 20130510. https://doi.org/10.1098/rstb.2013.0510.

23. Riau, A.K., Ong, H.S., Yam, G.H.F., and Mehta, J.S. (2019). Sustained Delivery System for Stem Cell-Derived Exosomes. Frontiers in Pharmacology *10*.

24. Herman, S., Fishel, I., and Offen, D. (2021). Intranasal delivery of mesenchymal stem cells-derived extracellular vesicles for the treatment of neurological diseases. STEM CELLS *39*, 1589–1600. https://doi.org/10.1002/stem.3456.

25. Zhang, K., and Cheng, K. (2023). Stem cell-derived exosome versus stem cell therapy. Nat Rev Bioeng, 1–2. https://doi.org/10.1038/s44222-023-00064-2.

26. Tan, F., Li, X., Wang, Z., Li, J., Shahzad, K., and Zheng, J. (2024). Clinical applications of stem cell-derived exosomes. Signal Transduction and Targeted Therapy *9*, 17. https://doi.org/10.1038/s41392-023-01704-0.

27. Tripathi, M.K., Ojha, S.K., Kartawy, M., Hamoudi, W., Choudhary, A., Stern, S., Aran, A., and Amal, H. (2023). The NO Answer for Autism Spectrum Disorder. Advanced Science *10*, 2205783. https://doi.org/10.1002/advs.202205783.

28. Brennand, K.J., Simone, A., Jou, J., Gelboin-Burkhart, C., Tran, N., Sangar, S., Li, Y., Mu, Y., Chen, G., Yu, D., et al. (2011). Modelling schizophrenia using human induced pluripotent stem cells. Nature *473*, 221–225. https://doi.org/10.1038/nature09915.

29. Théry, C., Amigorena, S., Raposo, G., and Clayton, A. (2006). Isolation and characterization of exosomes from cell culture supernatants and biological fluids. Curr Protoc Cell Biol *Chapter 3*, Unit 3.22. https://doi.org/10.1002/0471143030.cb0322s30.

30. Perets, N., Hertz, S., London, M., and Offen, D. (2018). Intranasal administration of exosomes derived from mesenchymal stem cells ameliorates autistic-like behaviors of BTBR mice. Mol Autism *9*, 57. https://doi.org/10.1186/s13229-018-0240-6.

31. Zinger, A., Cvetkovic, C., Sushnitha, M., Naoi, T., Baudo, G., Anderson, M., Shetty, A., Basu, N., Covello, J., Tasciotti, E., et al. (2021). Humanized Biomimetic Nanovesicles for Neuron Targeting. Adv Sci (Weinh) *8*, e2101437. https://doi.org/10.1002/advs.202101437.

32. Perets, N., Oron, O., Herman, S., Elliott, E., and Offen, D. (2020). Exosomes derived from mesenchymal stem cells improved core symptoms of genetically modified mouse model of autism Shank3B. Molecular Autism *11*, 65. https://doi.org/10.1186/s13229-020-00366-x.

33. Stern, S., Santos, R., Marchetto, M.C., Mendes, A.P.D., Rouleau, G.A., Biesmans, S., Wang, Q.W., Yao, J., Charnay, P., Bang, A.G., et al. (2018). Neurons derived from patients with bipolar disorder divide into intrinsically different sub-populations of neurons, predicting the patients' responsiveness to lithium. Mol Psychiatry *23*, 1453–1465. https://doi.org/10.1038/mp.2016.260.

34. Stern, S., Sarkar, A., Galor, D., Stern, T., Mei, A., Stern, Y., Mendes, A.P.D., Randolph-Moore, L., Rouleau, G., Bang, A.G., et al. (2020). A Physiological Instability Displayed in Hippocampal Neurons Derived From Lithium-Nonresponsive Bipolar Disorder Patients. Biol Psychiatry *88*, 150–158. https://doi.org/10.1016/j.biopsych.2020.01.020.

35. Fonseka, P., Pathan, M., Chitti, S.V., Kang, T., and Mathivanan, S. (2021). FunRich enables enrichment analysis of OMICs datasets. Journal of Molecular Biology *433*, 166747. https://doi.org/10.1016/j.jmb.2020.166747.

36. Pathan, M., Keerthikumar, S., Chisanga, D., Alessandro, R., Ang, C.-S., Askenase, P., Batagov, A.O., Benito-Martin, A., Camussi, G., Clayton, A., et al. (2017). A novel community driven

software for functional enrichment analysis of extracellular vesicles data. Journal of Extracellular Vesicles *6*, 1321455. https://doi.org/10.1080/20013078.2017.1321455.

37. Yilmaz, S. Volcano plot (https://www.mathworks.com/matlabcentral/fileexchange/133987-volcano-plot), MATLAB Central File Exchange. Retrieved August 18, 2024.

38. Tsivion-Visbord, H., Perets, N., Sofer, T., Bikovski, L., Goldshmit, Y., Ruban, A., and Offen, D. (2020). Mesenchymal stem cells derived extracellular vesicles improve behavioral and biochemical deficits in a phencyclidine model of schizophrenia. Translational Psychiatry *10*, 305. https://doi.org/10.1038/s41398-020-00988-y.

39. Schafer, S.T., Paquola, A.C.M., Stern, S., Gosselin, D., Ku, M., Pena, M., Kuret, T.J.M., Liyanage, M., Mansour, A.A., Jaeger, B.N., et al. (2019). Pathological priming causes developmental gene network heterochronicity in autistic subject-derived neurons. Nature Neuroscience *22*, 243–255. https://doi.org/10.1038/s41593-018-0295-x.

40. Deneault, E., Faheem, M., White, S.H., Rodrigues, D.C., Sun, S., Wei, W., Piekna, A., Thompson, T., Howe, J.L., Chalil, L., et al. (2019). CNTN5-/+or EHMT2-/+human iPSC-derived neurons from individuals with autism develop hyperactive neuronal networks. eLife *8*, e40092. https://doi.org/10.7554/eLife.40092.

41. Avazzadeh, S., Quinlan, L.R., Reilly, J., McDonagh, K., Jalali, A., Wang, Y., McInerney, V., Krawczyk, J., Ding, Y., Fitzgerald, J., et al. (2021). NRXN1α(+/-) is associated with increased excitability in ASD iPSC-derived neurons. BMC Neurosci *22*, 56. https://doi.org/10.1186/s12868-021-00661-0.

42. Brant, B., Stern, T., Shekhidem, H.A., Mizrahi, L., Rosh, I., Stern, Y., Ofer, P., Asleh, A., Umanah, G.K.E., Jada, R., et al. (2021). IQSEC2 mutation associated with epilepsy, intellectual disability, and autism results in hyperexcitability of patient-derived neurons and deficient synaptic transmission. Mol Psychiatry *26*, 7498–7508. https://doi.org/10.1038/s41380-021-01281-0.

43. Supekar, K., Uddin, L.Q., Khouzam, A., Phillips, J., Gaillard, W.D., Kenworthy, L.E., Yerys, B.E., Vaidya, C.J., and Menon, V. (2013). Brain hyperconnectivity in children with autism and its links to social deficits. Cell Rep *5*, 738–747. https://doi.org/10.1016/j.celrep.2013.10.001.

44. Tang, G., Gudsnuk, K., Kuo, S.-H., Cotrina, M.L., Rosoklija, G., Sosunov, A., Sonders, M.S., Kanter, E., Castagna, C., Yamamoto, A., et al. (2014). Loss of mTOR-Dependent Macroautophagy Causes Autistic-like Synaptic Pruning Deficits. Neuron *83*, 1131–1143. https://doi.org/10.1016/j.neuron.2014.07.040.

45. Romanovsky, E., Choudhary, A., Peles, D., Akel, A.A., and Stern, S. (2023). Uncovering convergence and divergence between autism and schizophrenia using genomic tools and patients' neurons. bioRxiv, 2023.08.11.552921. https://doi.org/10.1101/2023.08.11.552921.

46. Haraszti, R.A., Didiot, M.-C., Sapp, E., Leszyk, J., Shaffer, S.A., Rockwell, H.E., Gao, F., Narain, N.R., DiFiglia, M., Kiebish, M.A., et al. (2016). High-resolution proteomic and lipidomic analysis of exosomes and microvesicles from different cell sources. Journal of Extracellular Vesicles *5*, 32570. https://doi.org/10.3402/jev.v5.32570.

47. Lee, Y.J., Shin, K.J., and Chae, Y.C. (2024). Regulation of cargo selection in exosome biogenesis and its biomedical applications in cancer. Experimental & Molecular Medicine *56*, 877–889. https://doi.org/10.1038/s12276-024-01209-y.

48. Korkut, C., Ataman, B., Ramachandran, P., Ashley, J., Barria, R., Gherbesi, N., and Budnik, V. (2009). Trans-Synaptic Transmission of Vesicular Wnt Signals through Evi/Wntless. Cell *139*, 393–404. https://doi.org/10.1016/j.cell.2009.07.051.

49. Korkut, C., Li, Y., Koles, K., Brewer, C., Ashley, J., Yoshihara, M., and Budnik, V. (2013). Regulation of Postsynaptic Retrograde Signaling by Presynaptic Exosome Release. Neuron *77*, 1039–1046. https://doi.org/10.1016/j.neuron.2013.01.013.

50. Khatami, S.H., Karami, N., Taheri-Anganeh, M., Taghvimi, S., Tondro, G., Khorsand, M., Soltani Fard, E., Sedighimehr, N., Kazemi, M., Rahimi Jaberi, K., et al. (2023). Exosomes: Promising Delivery Tools for Overcoming Blood-Brain Barrier and Glioblastoma Therapy. Molecular Neurobiology *60*, 4659–4678. https://doi.org/10.1007/s12035-023-03365-0.

51. Bruno, S., Grange, C., Deregibus, M.C., Calogero, R.A., Saviozzi, S., Collino, F., Morando, L., Busca, A., Falda, M., Bussolati, B., et al. (2009). Mesenchymal Stem Cell-Derived Microvesicles Protect Against Acute Tubular Injury. Journal of the American Society of Nephrology *20*.

52. Bonab, M.M., Alimoghaddam, K., Talebian, F., Ghaffari, S.H., Ghavamzadeh, A., and Nikbin, B. (2006). Aging of mesenchymal stem cell in vitro. BMC Cell Biology *7*, 14. https://doi.org/10.1186/1471-2121-7-14.

53. Binato, R., de Souza Fernandez, T., Lazzarotto-Silva, C., Du Rocher, B., Mencalha, A., Pizzatti, L., Bouzas, L.F., and Abdelhay, E. (2013). Stability of human mesenchymal stem cells during in vitro culture: considerations for cell therapy. Cell Prolif *46*, 10–22. https://doi.org/10.1111/cpr.12002.

54. Yang, Y.-H.K., Ogando, C.R., Wang See, C., Chang, T.-Y., and Barabino, G.A. (2018). Changes in phenotype and differentiation potential of human mesenchymal stem cells aging in vitro. Stem Cell Research & Therapy *9*, 131. https://doi.org/10.1186/s13287-018-0876-3.

55. Mastrolia, I., Foppiani, E.M., Murgia, A., Candini, O., Samarelli, A.V., Grisendi, G., Veronesi, E., Horwitz, E.M., and Dominici, M. (2019). Challenges in Clinical Development of Mesenchymal Stromal/Stem Cells: Concise Review. Stem Cells Transl Med *8*, 1135–1148. https://doi.org/10.1002/sctm.19-0044.

56. Cerneckis, J., Cai, H., and Shi, Y. (2024). Induced pluripotent stem cells (iPSCs): molecular mechanisms of induction and applications. Signal Transduction and Targeted Therapy *9*, 112. https://doi.org/10.1038/s41392-024-01809-0.

57. Mizrahi, L., Choudhary, A., Ofer, P., Goldberg, G., Milanesi, E., Kelsoe, J.R., Gurwitz, D., Alda, M., Gage, F.H., and Stern, S. (2023). Immunoglobulin genes expressed in lymphoblastoid cell lines discern and predict lithium response in bipolar disorder patients. Molecular Psychiatry. https://doi.org/10.1038/s41380-023-02183-z.

58. Nassar, L.R., Barber, G.P., Benet-Pagès, A., Casper, J., Clawson, H., Diekhans, M., Fischer, C., Gonzalez, J.N., Hinrichs, A.S., Lee, B.T., et al. (2023). The UCSC Genome Browser database: 2023 update. Nucleic Acids Res *51*, D1188–D1195. https://doi.org/10.1093/nar/gkac1072.

Figure legends

Figure 1. Cortical neuron differentiation from Control and *Shank3* (c3679insG) iPSC lines and exosomes isolation & characterization

a) An illustration of a frameshift mutation in the *Shank3* (c3679insG) gene causing PMS and ASD symptoms in a female child[13].
b) A snapshot of the UCSC browser[58] for the human *Shank3* gene coordinates at Chromosome 22 and NCBI ref-seq gene architecture using hg38 genome assembly.
c) *Shank3* single-cell RNA sequencing data plotted for the fetal and adult human brain. The data was obtained from the single-cell RNA expression track settings (publicly available, last updated on 2022-04-11) from the UCSC browser[58].
d) Schematics for cortical differentiation from control and *Shank3* human iPSCs by differentiation into embryoid bodies (EBs), neural progenitor cells(NPCs), and then into cortical neurons. The cortical differentiation from NPCs was done for 29-31 days.
e) The exosome isolation procedure used in the study included differential centrifugation to remove, dead cells and debris from the conditioned media from control and *shank3* neurons followed by ultracentrifugation. *For details, see methods*.
f) Exosome size and zeta potential quantification by Zetasizer™ using dynamic light scattering method.
g) Micrograph for uptake of PKH-67 labeled exosomes by cortical neuron derived from a control iPSC lines.

Figure 2. Control cortical neurons similar to *Shank3* neurons display hyperexcitability, and a high spontaneous firing rate when treated with *Shank3* neuron-derived exosomes.

a) Exosomes were isolated from the control neuron and *Shank3* neuron and the purified exosome was exchanged i.e., control neurons were treated with shank3 neuron exosomes and vice-versa, and the functional analysis of neurons was performed by whole-cell patch-clamp technique.
b) Immunocytochemistry images of TBR1 (green), CTIP2 (purple), MAP2 (red), and DAPI (blue)for (i) untreated control neurons, (ii) control neurons treated with *Shank3* neuron-derived exosomes. The exosomes were added two times (see methods) (iii) control neurons treated with synthetic liposomes.
c) Na+/K+ currents example traces as observed in control cortical neurons after 28-30 days of differentiation by whole cell patch clamp technique.
d) Na+/K+ currents example traces as observed in control cortical neurons treated with Shank3 neuron-derived exosomes (three times) after 28-30 days of differentiation by whole cell patch clamp technique.
e) Na+/K+ currents example traces as observed in control cortical neurons treated with synthetic liposomes after 28-30 days of differentiation by whole cell patch clamp technique.
f) The average Na+ currents recorded in the control (green), control treated with shank3 neuron exosomes (light blue) and, control treated with synthetic liposomes (dark green) after 28-30 days of differentiation by whole cell patch clamp.
g) The average Slow K+ currents were recorded in the control (green), control treated with shank3 neuron exosomes (light blue) and, control treated with synthetic liposomes (dark green) after 28-30 days of differentiation by whole cell patch clamp.

h) The average Slow K+ currents recorded in the control (green), control treated with shank3 neuron exosomes (light blue) and, control treated with synthetic liposomes (dark green) after 28-30 days of differentiation by whole cell patch clamp.
i) Total evoked potential example traces as observed in control cortical neurons after 28-30 days of differentiation by whole cell patch clamp technique.
j) Total evoked potential example traces as observed in control cortical neurons treated with Shank3 neuron-derived exosomes (three times) after 28-30 days of differentiation by whole cell patch clamp technique.
k) Total evoked potential example traces as observed in control cortical neurons treated with synthetic liposomes after 28-30 days of differentiation by whole cell patch clamp technique.
l) Violin plot for the total evoked potential for control (green), control treated with shank3 neuron exosomes (light blue) and, control treated with synthetic liposomes (dark green). *$p<0.05$, **$p<0.01$. *Mann Whitney U test*
m) Spontaneous firing rate example traces as observed in control cortical neurons after 28-30 days of differentiation by whole cell patch clamp technique.
n) Spontaneous firing rate example traces as observed in control cortical neurons treated with Shank3 neuron-derived exosomes (three times) after 28-30 days of differentiation by whole cell patch clamp technique.
o) Spontaneous firing rate example traces as observed in control cortical neurons treated with synthetic liposomes after 28-30 days of differentiation by whole cell patch clamp technique.
p) Violin plot for the Spontaneous firing rate control (green), control treated with shank3 neuron exosomes (light blue), and, control treated with synthetic liposomes (dark green). *$p<0.05$, **$p<0.01$. *Mann Whitney U test*
q) EPSCs rate example traces as observed in control cortical neurons different after 28-30 days of differentiation by whole cell patch clamp technique.
r) EPSCs rate example traces as observed in control cortical neurons treated with Shank3 neuron-derived exosomes (three times) after 28-30 days of differentiation by whole cell patch clamp technique.
s) EPSCs rate example traces as observed in control cortical neurons treated with synthetic liposomes after 28-30 days of differentiation by whole cell patch clamp technique.
t) Violin plot for the EPSCs rate control (green), control treated with shank3 neuron exosomes (light blue), and, control treated with synthetic liposomes (dark green). *$p<0.05$, **$p<0.01$. *Mann Whitney U test*
u) Violin plot for the EPSCs amplitude control (green), control treated with shank3 neuron exosomes (light blue), and, control treated with synthetic liposomes (dark green). *$p<0.05$, **$p<0.01$. *Mann Whitney U test*

Figure 3. *Shank3* cortical neurons maintain hyperexcitability, increased Na+/K+ currents, high spontaneous firing rate, and EPSCs rate even after treatment with control neuron-derived exosomes

a) Immunocytochemistry images of TBR1 (green), CTIP2 (purple) , and MAP2 (red), DAPI (blue)for (i) untreated Shank3 neurons, (ii) Shank3 neurons treated with control neuron-derived exosomes. The exosomes were added two times. (see methods)
b) Na+/K+ currents example traces as observed in shank3 cortical neurons after 28-30 days of differentiation measured by whole cell patch clamp technique.

c) Na+/K+ currents example traces as observed in shank3 cortical neurons treated with control neuron derived exosomes (three times) after 28-30 days of differentiation measured by whole cell patch clamp technique.
d) The average Na+ currents recorded in shank3 (red) , shank3 treated with control neuron exosomes (orange) after 28-30 days of differentiation by whole cell patch clamp.
e) The average Slow K+ currents recorded in shank3 (red) , shank3 treated with control neuron exosomes (orange) after 28-30 days of differentiation by whole cell patch clamp.
f) The average fast K+ currents recorded in shank3 (red) , shank3 treated with control neuron exosomes (orange) after 28-30 days of differentiation by whole cell patch clamp.
g) Total evoked potential was recorded in shank3 (red) and, shank3 treated with control neuron exosomes (orange) after 28-30 days of differentiation by whole cell patch clamp.
h) Total evoked potential recorded in shank3 (red) , shank3 treated with control neuron exosomes (orange) after 28-30 days of differentiation by whole cell patch clamp.
i) Violin plot for the total evoked potential for shank3 (red) , shank3 treated with control neuron exosomes (orange) . *p<0.05, **p<0.01. NS: not significant *Mann Whitney U test*
j) Spontaneous firing rate recorded in shank3 (red) , shank3 treated with control neuron exosomes (orange) after 28-30 days of differentiation by whole cell patch clamp.
k) Spontaneous firing rate recorded in shank3 (red) , shank3 treated with control neuron exosomes (orange) after 28-30 days of differentiation by whole cell patch clamp.
l) Violin plot for the for Spontaneous firing rate for shank3 (red) , shank3 treated with control neuron exosomes (orange) . *p<0.05, **p<0.01. NS: not significant *Mann Whitney U test.*
m) EPSCs rate example traces as observed in shank3 (red) , shank3 treated with control neuron exosomes (orange) after 28-30 days of differentiation by whole cell patch clamp.
n) EPSCs rate example traces as observed in shank3 (red) , shank3 treated with control neuron exosomes (orange) after 28-30 days of differentiation by whole cell patch clamp.
o) Violin plot for the EPSCs rate shank3 (red) , shank3 treated with control neuron exosomes (orange) after 28-30 days of differentiation by whole cell patch clamp. *p<0.05, **p<0.01. NS: not significant *Mann Whitney U test.*
p) Violin plot for the EPSCs amplitude shank3 (red), shank3 treated with control neuron exosomes (orange) after 28-30 days of differentiation by whole cell patch clamp. *p<0.05, **p<0.01. NS: not significant *Mann Whitney U test.*

Figure 4. Mesenchymal stem-cell-derived exosomes rescue the hyper-excitability, increased Na+/K+ currents, and EPSCs rate in *Shank3* cortical neurons.

a) A schematic demonstrating the isolation of exosomes from the conditioned media of the mesenchymal stem cell (MSC) culture and treatment of the Shank3 mutant cortical neurons with shank3 neurons with MSC-Exo from the start of the differentiation. The treatment with MSC exo was done 3 times during the cortical differentiation timeline. The electrophysiological parameters were measured using the whole cell patch clamp technique at 29-31 days of differentiation.
b) Size and zeta potential characterization of MSC-exo by dynamic light scattering.
c) Immunocytochemistry images of TBR1 (green), CTIP2 (purple), and MAP2 (red), DAPI (blue) for (i) untreated control neurons, (ii) Shank3 neurons treated with MSC derived exosomes. The exosomes were added three times every 8-9 days
d) Na+/K+ currents example traces as observed in shank3 cortical neurons after 28-30 days of differentiation measured by whole cell patch clamp technique.

e) Na+/K+ currents example traces as observed in shank3 cortical neurons treated with MSC-derived exosomes (three times) after 28-30 days of differentiation measured by whole cell patch clamp technique.
f) The average Na+ currents recorded in shank3 (red), shank3 treated with MSC-derived exosomes (orange) after 28-30 days of differentiation by whole cell patch clamp.
g) The average Slow K+ currents recorded in shank3 (red), shank3 treated with MSC-derived exosomes (orange) after 28-30 days of differentiation by whole cell patch clamp.
h) The average Fast K+ currents recorded in shank3 (red) , shank3 treated with MSC-derived exosomes (orange) after 28-30 days of differentiation by whole cell patch clamp.
i) Total evoked potential recorded in shank3 (red) , shank3 treated with MSC-derived exosomes (orange) after 28-30 days of differentiation by whole cell patch clamp.
j) Total evoked potential recorded in shank3 (red) , shank3 treated with MSC-derived exosomes (orange) after 28-30 days of differentiation by whole cell patch clamp.
k) Violin plot for the total evoked potential for shank3 (red) , shank3 treated with MSC-derived exosomes (orange) . *$p<0.05$, **$p<0.01$. NS: not significant *Mann Whitney U test*
l) Spontaneous firing rate recorded in shank3 (red) , shank3 treated with MSC-derived exosomes (orange) after 28-30 days of differentiation by whole cell patch clamp.
m) Spontaneous firing rate recorded in shank3 (red) , shank3 treated with MSC-derived exosomes (orange) after 28-30 days of differentiation by whole cell patch clamp.
n) Violin plot for the for Spontaneous firing rate for shank3 (red) , shank3 treated with MSC-derived exosomes (orange) . *$p<0.05$, **$p<0.01$. NS: not significant *Mann Whitney U test.*
o) EPSCs rate example traces as observed in shank3 (red) , shank3 treated with MSC-derived exosomes (orange) after 28-30 days of differentiation by whole cell patch clamp.
p) EPSCs rate example traces as observed shank3 (red) , shank3 treated with MSC-derived exosomes (orange) after 28-30 days of differentiation by whole cell patch clamp.
q) Violin plot for the for EPSCs rate shank3 (red) , shank3 treated with MSC derived exosomes (orange) after 28-30 days of differentiation by whole cell patch clamp. *$p<0.05$, **$p<0.01$. NS: not significant *Mann Whitney U test.*
r) Violin plot for the for EPSCs amplitude shank3 (red) , shank3 treated with MSC derived exosomes (orange) after 28-30 days of differentiation by whole cell patch clamp. *$p<0.05$, **$p<0.01$. NS: not significant *Mann Whitney U test.*

Figure 5. iPSC-derived exosomes rescue the hyper-excitability, increased Na+/K+ currents, and high spontaneous firing rate in *Shank3* cortical neurons.

a) A schematic demonstrating the isolation of exosomes from the conditioned media of the induced pluripotent stem cell (iPSC) culture and treatment of the Shank3 mutant cortical neurons with shank3 neurons with iPSC-Exo from the start of the differentiation. The treatment with iPSC exo was done 3 times during the cortical differentiation timeline. The electrophysiological parameters were measured using whole cell patch clamp technique at 29-31 days of differentiation.
b) Size and zeta potential characterization of MSC-exo by dynamic light scattering.
c) Immunocytochemistry images of TBR1 (green), CTIP2 (purple), MAP2 (red), DAPI (blue) for (i) untreated control neurons, (ii) Shank3 neurons treated with iPSC derived exosomes. The exosomes were added three times every 8-9 days
d) Na+/K+ currents example traces as observed in shank3 cortical neurons after 28-30 days of differentiation measured by whole cell patch clamp technique.

e) Na+/K+ currents example traces as observed in shank3 cortical neurons treated with iPSC-derived exosomes (three times) after 28-30 days of differentiation measured by whole cell patch clamp technique.
f) The average Na+ currents recorded in shank3 (red), shank3 treated with iPSC-derived exosomes (orange) after 28-30 days of differentiation by whole cell patch clamp.
g) The average slow K+ currents recorded in shank3 (red) , and shank3 treated with iPSC-derived exosomes (orange) after 28-30 days of differentiation by whole cell patch clamp.
h) The average fast K+ currents recorded in shank3 (red) , and shank3 treated with iPSC-derived exosomes (orange) after 28-30 days of differentiation by whole cell patch clamp.
i) Total evoked potential recorded in shank3 (red) , shank3 treated with iPSC-derived exosomes (orange) after 28-30 days of differentiation by whole cell patch clamp.
j) Total evoked potential recorded in shank3 (red) , shank3 treated with iPSC-derived exosomes (orange) after 28-30 days of differentiation by whole cell patch clamp.
k) Violin plot for the total evoked potential for shank3 (red) , shank3 treated with iPSC-derived exosomes (orange) . *$p<0.05$, **$p<0.01$. NS: not significant *Mann Whitney U test*
l) Spontaneous firing rate recorded in shank3 (red) , shank3 treated with iPSC-derived exosomes (orange) after 28-30 days of differentiation by whole cell patch clamp.
m) Spontaneous firing rate recorded in shank3 (red) , shank3 treated with iPSC-derived exosomes (orange) after 28-30 days of differentiation by whole cell patch clamp.
n) Violin plot for the for Spontaneous firing rate for shank3 (red) , shank3 treated with iPSC-derived exosomes (orange) . *$p<0.05$, **$p<0.01$. NS: not significant *Mann whitney U test.*
o) EPSCs rate example traces as observed in shank3 (red) , shank3 treated with iPSC-derived exosomes (orange) after 28-30 days of differentiation by whole cell patch clamp.
p) EPSCs rate example traces as observed shank3 (red) , shank3 treated with iPSC-derived exosomes (orange) after 28-30 days of differentiation by whole cell patch clamp.
q) Violin plot for the for EPSCs rate shank3 (red) , shank3 treated with iPSC derived exosomes (orange) after 28-30 days of differentiation by whole cell patch clamp. *$p<0.05$, **$p<0.01$. NS: not significant *Mann whitney U test.*
r) Violin plot for the for EPSCs amplitude shank3 (red) , shank3 treated iPSC derived exosomes (orange) after 28-30 days of differentiation by whole cell patch clamp. *$p<0.05$, **$p<0.01$. NS: not significant *Mann Whitney U test.*

Figure 6. Proteomic analysis of the Control neuron exosomes, *Shank3* neuron exosomes, MSC exosomes, and iPSC exosomes.

a) A Venn diagram visualization of identified proteins as well as their overlap in Control neuron exosomes, *Shank3* neuron exosomes, MSC exosomes, and iPSC exosomes using LC-MS/MS.
b) The cellular component analysis of the identified proteins from four exosomes: neuron-derived (control and shank3) and stem cell-derived (MSC and iPSC) exosomes.
c) The volcano plot displaying the differentially expressed proteins identified between shank3 and control neuron-derived exosomes.
d) The biological process analysis of the identified proteins between shank3 and control neuron-derived exosomes.
e) The volcano plot displaying the differentially expressed proteins identified between control neuron-derived exosomes and MSC-derived exosomes.
f) The biological process analysis of the identified proteins between control neuron-derived exosomes and MSC-derived exosomes.

g) The volcano plot displaying the differentially expressed proteins identified between control neuron-derived exosomes and iPSC-derived exosomes.
h) The biological process analysis of the identified proteins between control neuron-derived exosomes and iPSC-derived exosomes.
i) The volcano plot displaying the differentially expressed proteins identified between MSC-derived exosomes and iPSC-derived exosomes.
j) The biological process analysis of the identified proteins between MSC-derived exosomes and iPSC-derived exosomes.

All the analysis except the volcano plot for differentially expressed proteins were done using FunRich proteomicsw software[35].

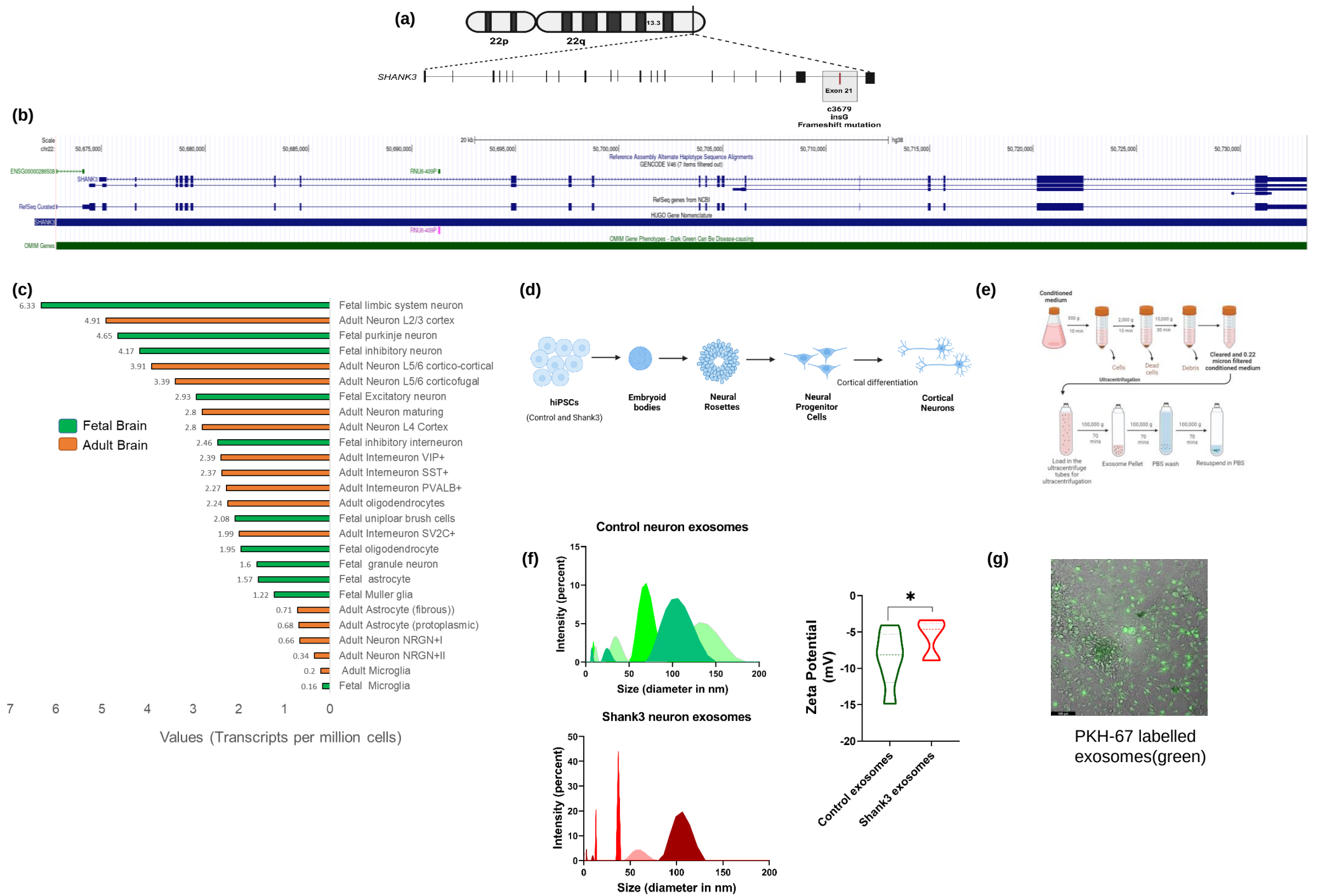
(a)
22p
22q
13.3
SHANK3
Exon 21
c3679
insG
Frameshift mutation
(b)
(c)
Fetal Brain
Adult Brain
Fetal limbic system neuron 6.33
Adult Neuron L2/3 cortex 4.91
Fetal purkinje neuron 4.65
Fetal inhibitory neuron 4.17
Adult Neuron L5/6 cortico-cortical 3.91
Adult Neuron L5/6 corticofugal 3.39
Fetal Excitatory neuron 2.93
Adult Neuron maturing 2.8
Adult Neuron L4 Cortex 2.8
Fetal inhibitory interneuron 2.46
Adult Interneuron VIP+ 2.39
Adult Interneuron SST+ 2.37
Adult Interneuron PVALB+ 2.27
Adult oligodendrocytes 2.24
Fetal uniploar brush cells 2.08
Adult Interneuron SV2C+ 1.99
Fetal oligodendrocyte 1.95
Fetal granule neuron 1.6
Fetal astrocyte 1.57
Fetal Muller glia 1.22
Adult Astrocyte (fibrous)) 0.71
Adult Astrocyte (protoplasmic) 0.68
Adult Neuron NRGN+I 0.66
Adult Neuron NRGN+II 0.34
Adult Microglia 0.2
Fetal Microglia 0.16
7 6 5 4 3 2 1 0
Values (Transcripts per million cells)
(d)
hiPSCs
(Control and Shank3)
Embryoid bodies
Neural Rosettes
Neural Progenitor Cells
Cortical differentiation
Cortical Neurons
(e)
Conditioned medium
Cells
Dead cells
Debris
Cleared and 0.22 micron filtered conditioned medium
Ultracentrifugation
Load in the ultracentrifuge tubes for ultracentrifugation
Exosome Pellet
PBS wash
Resuspend in PBS
(f)
Control neuron exosomes
Intensity (percent)
Size (diameter in nm)
Shank3 neuron exosomes
Intensity (percent)
Size (diameter in nm)
Zeta Potential (mV)
Control exosomes
Shank3 exosomes
(g)
PKH-67 labelled exosomes(green)

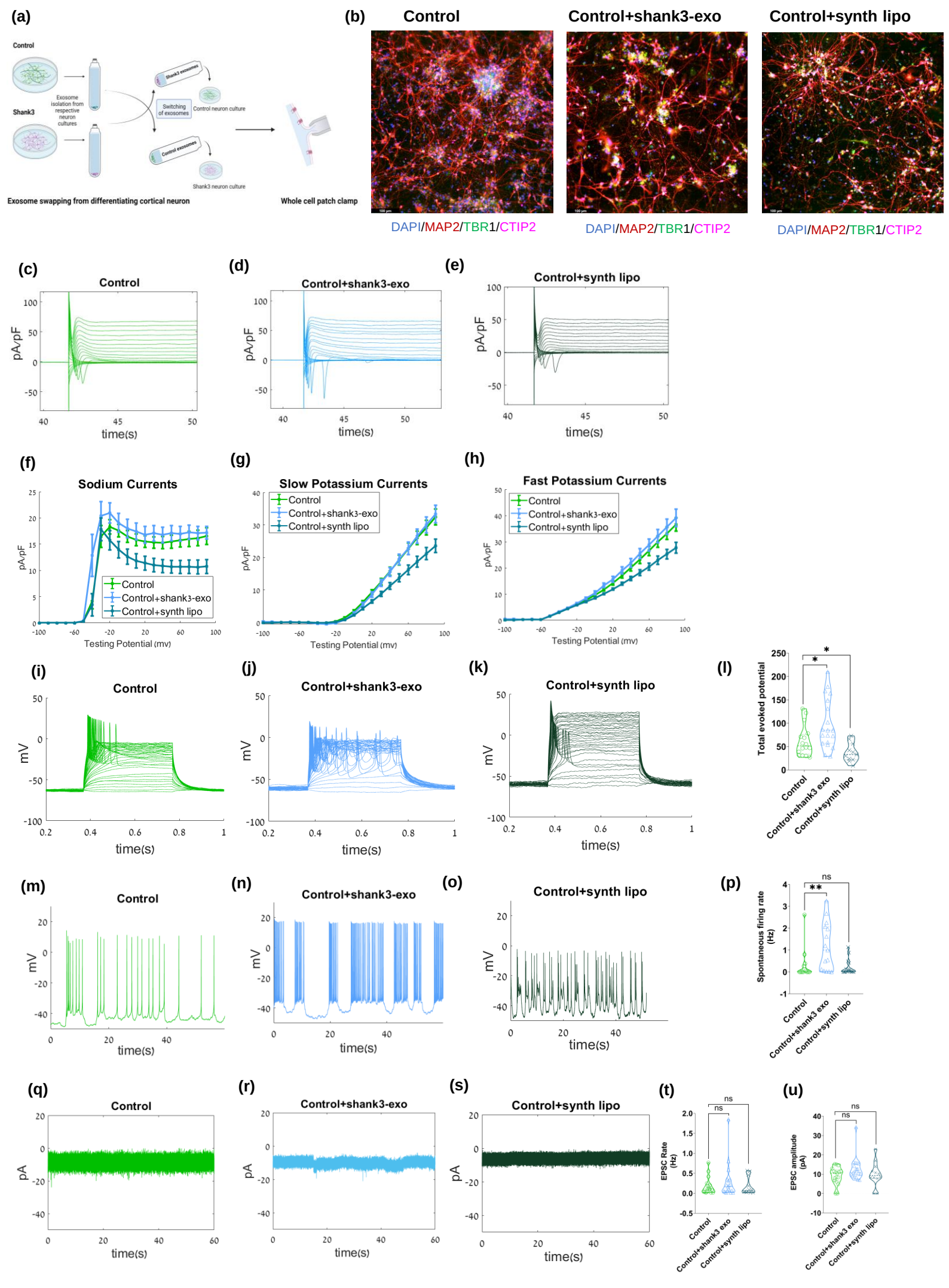
(a)
Control
Shank3
Exosome isolation from respective neuron cultures
Shank3 exosomes
Switching of exosomes
Control neuron culture
Control exosomes
Shank3 neuron culture
Exosome swapping from differentiating cortical neuron
Whole cell patch clamp
(b)
Control
Control+shank3-exo
Control+synth lipo
DAPI/MAP2/TBR1/CTIP2
DAPI/MAP2/TBR1/CTIP2
DAPI/MAP2/TBR1/CTIP2
(c)
Control
(d)
Control+shank3-exo
(e)
Control+synth lipo
pA/pF
time(s)
(f)
Sodium Currents
(g)
Slow Potassium Currents
(h)
Fast Potassium Currents
Control
Control+shank3-exo
Control+synth lipo
Testing Potential (mv)
(i)
Control
(j)
Control+shank3-exo
(k)
Control+synth lipo
mV
time(s)
(l)
Total evoked potential
Control
Control+shank3 exo
Control+synth lipo
(m)
Control
(n)
Control+shank3-exo
(o)
Control+synth lipo
(p)
Spontaneous firing rate (Hz)
ns
(q)
Control
(r)
Control+shank3-exo
(s)
Control+synth lipo
pA
(t)
EPSC Rate (Hz)
(u)
EPSC amplitude (pA)

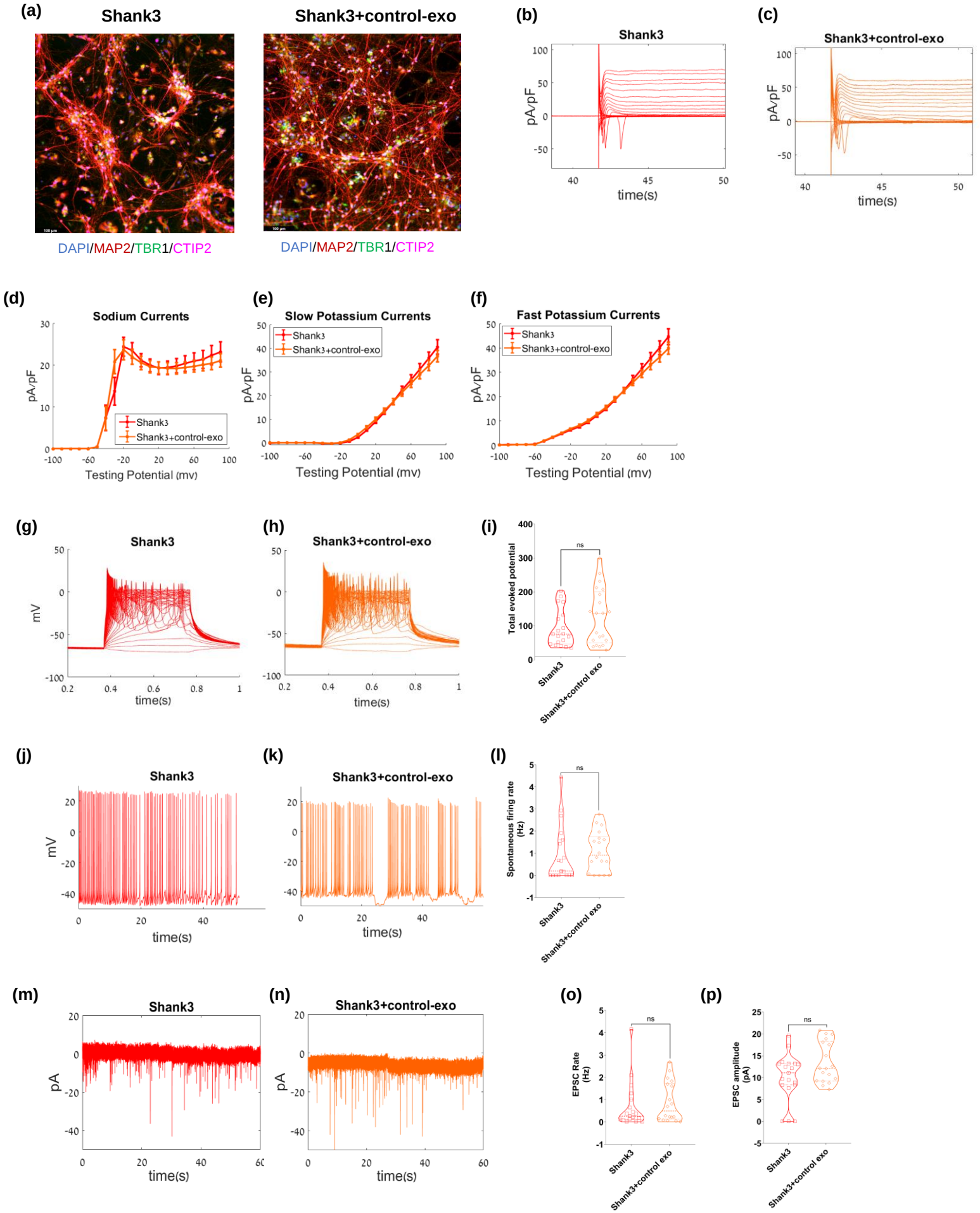
(a)
Shank3
Shank3+control-exo
DAPI/MAP2/TBR1/CTIP2
DAPI/MAP2/TBR1/CTIP2
(b)
Shank3
pA/pF
time(s)
(c)
Shank3+control-exo
pA/pF
time(s)
(d)
Sodium Currents
pA/pF
Testing Potential (mv)
Shank3
Shank3+control-exo
(e)
Slow Potassium Currents
pA/pF
Testing Potential (mv)
Shank3
Shank3+control-exo
(f)
Fast Potassium Currents
pA/pF
Testing Potential (mv)
Shank3
Shank3+control-exo
(g)
Shank3
mV
time(s)
(h)
Shank3+control-exo
time(s)
(i)
Total evoked potential
ns
Shank3
Shank3+control exo
(j)
Shank3
mV
time(s)
(k)
Shank3+control-exo
time(s)
(l)
Spontaneous firing rate (Hz)
ns
Shank3
Shank3+control exo
(m)
Shank3
pA
time(s)
(n)
Shank3+control-exo
pA
time(s)
(o)
EPSC Rate (Hz)
ns
Shank3
Shank3+control exo
(p)
EPSC amplitude (pA)
ns
Shank3
Shank3+control exo

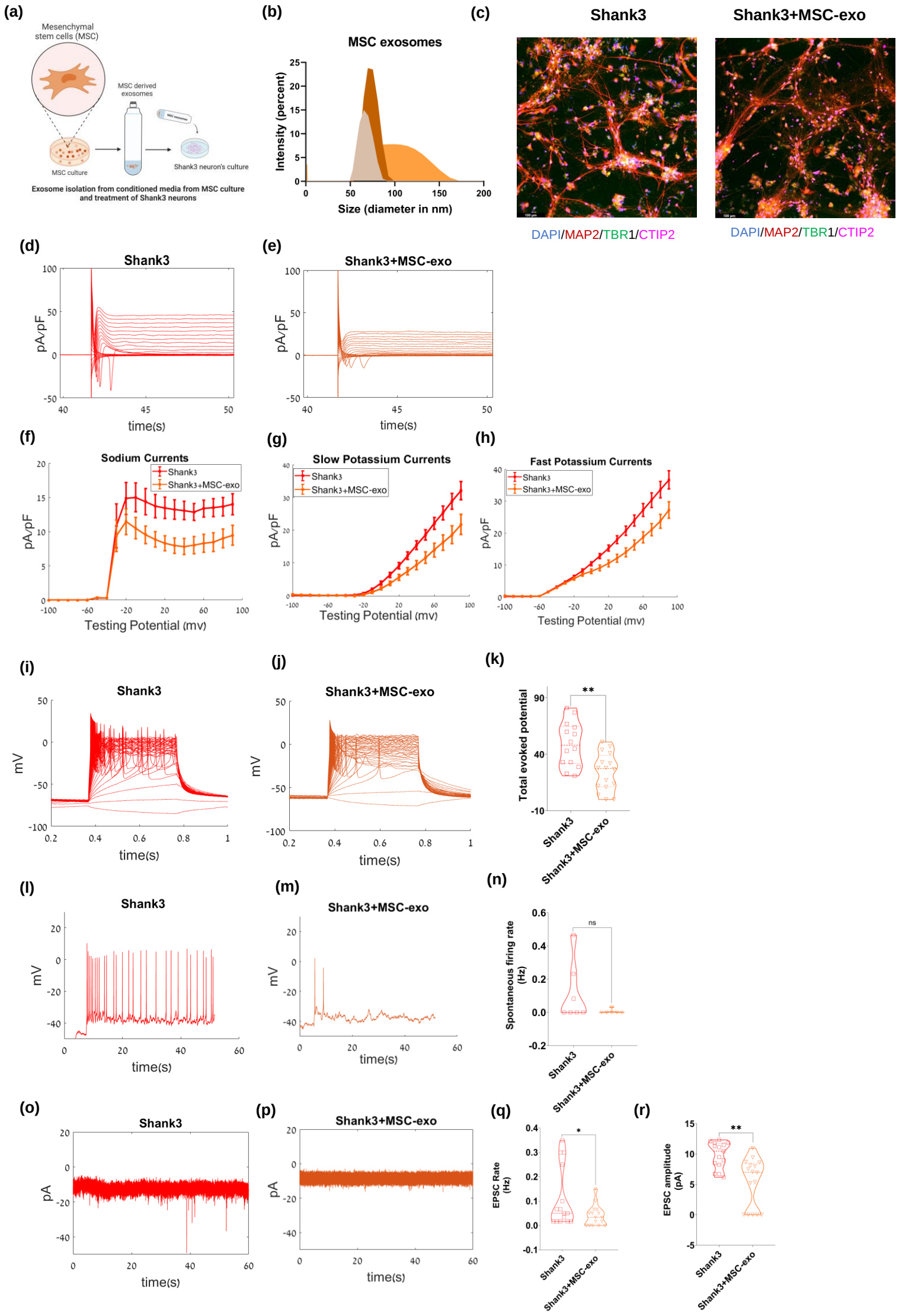
(a)
Mesenchymal stem cells (MSC)
MSC derived exosomes
MSC culture
Shank3 neuron's culture
Exosome isolation from conditioned media from MSC culture and treatment of Shank3 neurons
(b)
MSC exosomes
Intensity (percent)
Size (diameter in nm)
(c)
Shank3
Shank3+MSC-exo
DAPI/MAP2/TBR1/CTIP2
DAPI/MAP2/TBR1/CTIP2
(d)
Shank3
pA/pF
time(s)
(e)
Shank3+MSC-exo
pA/pF
time(s)
(f)
Sodium Currents
Shank3
Shank3+MSC-exo
pA/pF
Testing Potential (mv)
(g)
Slow Potassium Currents
Shank3
Shank3+MSC-exo
pA/pF
Testing Potential (mv)
(h)
Fast Potassium Currents
Shank3
Shank3+MSC-exo
pA/pF
Testing Potential (mv)
(i)
Shank3
mV
time(s)
(j)
Shank3+MSC-exo
mV
time(s)
(k)
Total evoked potential
**
Shank3
Shank3+MSC-exo
(l)
Shank3
mV
time(s)
(m)
Shank3+MSC-exo
mV
time(s)
(n)
Spontaneous firing rate (Hz)
ns
Shank3
Shank3+MSC-exo
(o)
Shank3
pA
time(s)
(p)
Shank3+MSC-exo
pA
time(s)
(q)
EPSC Rate (Hz)
*
Shank3
Shank3+MSC-exo
(r)
EPSC amplitude (pA)
**
Shank3
Shank3+MSC-exo

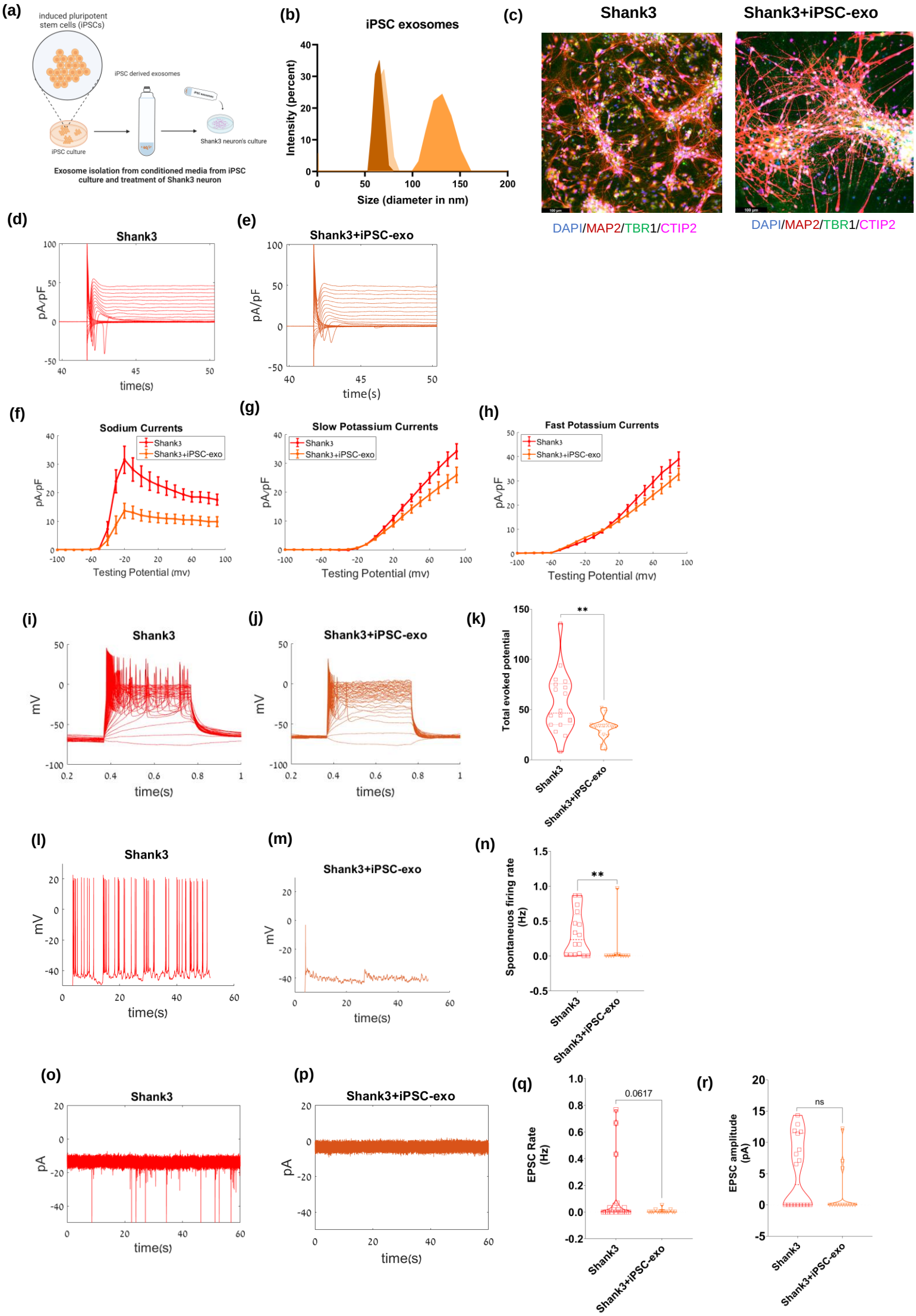
(a)
induced pluripotent stem cells (iPSCs)
iPSC derived exosomes
iPSC culture
Shank3 neuron's culture
Exosome isolation from conditioned media from iPSC culture and treatment of Shank3 neuron
(b)
iPSC exosomes
Intensity (percent)
Size (diameter in nm)
(c)
Shank3
Shank3+iPSC-exo
DAPI/MAP2/TBR1/CTIP2
DAPI/MAP2/TBR1/CTIP2
(d)
Shank3
pA/pF
time(s)
(e)
Shank3+iPSC-exo
pA/pF
time(s)
(f)
Sodium Currents
Shank3
Shank3+iPSC-exo
pA/pF
Testing Potential (mv)
(g)
Slow Potassium Currents
Shank3
Shank3+iPSC-exo
pA/pF
Testing Potential (mv)
(h)
Fast Potassium Currents
Shank3
Shank3+iPSC-exo
pA/pF
Testing Potential (mv)
(i)
Shank3
mV
time(s)
(j)
Shank3+iPSC-exo
mV
time(s)
(k)
Total evoked potential
**
Shank3
Shank3+iPSC-exo
(l)
Shank3
mV
time(s)
(m)
Shank3+iPSC-exo
mV
time(s)
(n)
Spontaneuos firing rate (Hz)
**
Shank3
Shank3+iPSC-exo
(o)
Shank3
pA
time(s)
(p)
Shank3+iPSC-exo
pA
time(s)
(q)
EPSC Rate (Hz)
0.0617
Shank3
Shank3+iPSC-exo
(r)
EPSC amplitude (pA)
ns
Shank3
Shank3+iPSC-exo

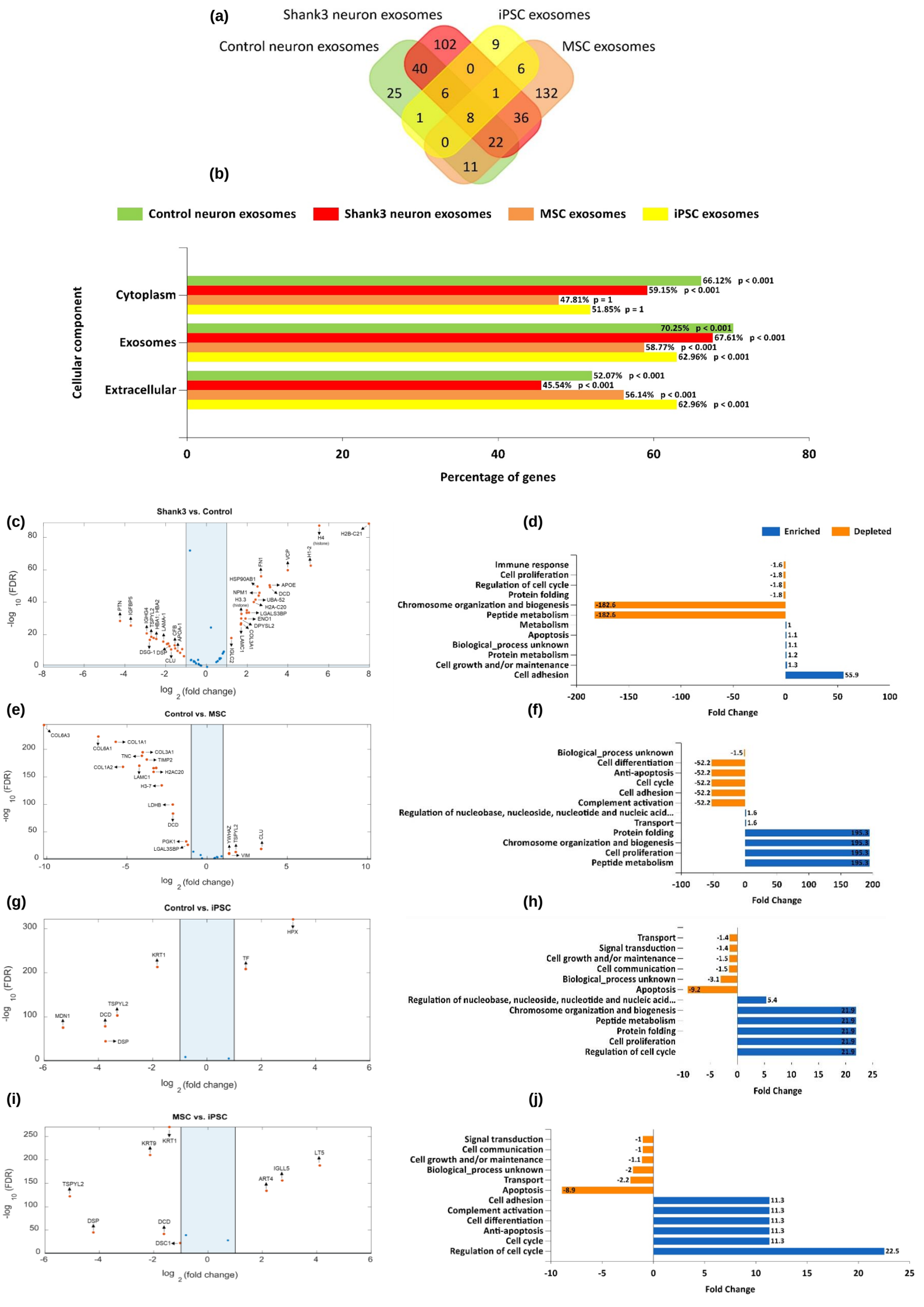
(a)
Shank3 neuron exosomes
iPSC exosomes
Control neuron exosomes
MSC exosomes
102
9
40
0
6
25
6
1
132
1
8
36
0
22
11
(b)
Control neuron exosomes
Shank3 neuron exosomes
MSC exosomes
iPSC exosomes
Cellular component
Cytoplasm
Exosomes
Extracellular
66.12% p < 0.001
59.15% p < 0.001
47.81% p = 1
51.85% p = 1
70.25% p < 0.001
67.61% p < 0.001
58.77% p < 0.001
62.96% p < 0.001
52.07% p < 0.001
45.54% p < 0.001
56.14% p < 0.001
62.96% p < 0.001
0
20
40
60
80
Percentage of genes
(c)
Shank3 vs. Control
-log 10 (FDR)
log 2 (fold change)
(d)
Enriched
Depleted
Immune response
Cell proliferation
Regulation of cell cycle
Protein folding
Chromosome organization and biogenesis
Peptide metabolism
Metabolism
Apoptosis
Biological_process unknown
Protein metabolism
Cell growth and/or maintenance
Cell adhesion
-1.6
-1.8
-1.8
-1.8
-182.6
-182.6
1
1.1
1.1
1.2
1.3
55.9
Fold Change
(e)
Control vs. MSC
-log 10 (FDR)
log 2 (fold change)
(f)
Biological_process unknown
Cell differentiation
Anti-apoptosis
Cell cycle
Cell adhesion
Complement activation
Regulation of nucleobase, nucleoside, nucleotide and nucleic acid...
Transport
Protein folding
Chromosome organization and biogenesis
Cell proliferation
Peptide metabolism
-1.5
-52.2
-52.2
-52.2
-52.2
-52.2
1.6
1.6
195.3
195.3
195.3
195.3
Fold Change
(g)
Control vs. iPSC
-log 10 (FDR)
log 2 (fold change)
(h)
Transport
Signal transduction
Cell growth and/or maintenance
Cell communication
Biological_process unknown
Apoptosis
Regulation of nucleobase, nucleoside, nucleotide and nucleic acid...
Chromosome organization and biogenesis
Peptide metabolism
Protein folding
Cell proliferation
Regulation of cell cycle
-1.4
-1.4
-1.5
-1.5
-3.1
-9.2
5.4
21.9
21.9
21.9
21.9
21.9
Fold Change
(i)
MSC vs. iPSC
-log 10 (FDR)
log 2 (fold change)
(j)
Signal transduction
Cell communication
Cell growth and/or maintenance
Biological_process unknown
Transport
Apoptosis
Cell adhesion
Complement activation
Cell differentiation
Anti-apoptosis
Cell cycle
Regulation of cell cycle
-1
-1
-1.1
-2
-2.2
-8.9
11.3
11.3
11.3
11.3
11.3
22.5
Fold Change